THE CONTENT OF UNITARITY CONSTRAINTS ON A POMERON POLE

WITH INTERCEPT ONE

J.L. Cardy [*] and A.R. White [+]

CERN -- Geneva

A B S T R A C T

We present a consistent picture of a Pomeron pole with intercept one, together with its cuts, which evades the decoupling arguments. We use the Reggeon cut discontinuity formulae to introduce Gribov's Reggeon calculus as an exact solution of multiparticle t channel unitarity. We show how, within the calculus, two-Pomeron iterations of a singular kernel can be responsible for the zero in the triple Pomeron vertex. Using the concept of a bare Pomeron pole as a multi-peripheral production process which is subsequently renormalized by other effects we apply the Reggeon calculus analysis to inclusive cross-sections. We find that the inclusive sum rule decoupling arguments are avoided because of the addition of enhanced absorptive corrections to the conventional Regge pole contributions. However, we show that in this picture the combined pole and two-Pomeron cut contribution to the total cross-section factorizes to order $(\log s)^{-2}$.

We also show that when the correct helicity structure of the Pomeron is taken into account the s channel unitarity condition for Pomeron scattering amplitudes does not lead to any serious decouplings.

----

[*] SRC Post-Doctoral Fellow.
    Address after 1st October 1973 : Daresbury Nuclear
    Physics Laboratory, Warrington, Lancs.

[+] Address after 1st October 1973 : N.A.L., P.O. Box
    500, Batavia, Ill. 60510.

1. INTRODUCTION

At the 1972 Chicago-Batavia Conference a picture was presented of a Pomeron Regge pole, with intercept one, in considerable theoretical difficulty. The reviews of Low[1] and Gribov[2] suggest that if the Pomeron is a simple Regge pole then it must decouple from a large number of processes in the forward direction[3]. The only essential difference in the pictures presented by Low and Gribov is that Gribov does not accept the Brower and Weis argument[4] that the Pomeron should actually decouple from total cross-sections. Gribov has the Pomeron decoupling from inelastic processes but argues for a cancellation mechanism which allows it to couple in total cross-sections. However, this cancellation mechanism requires all Pomeron couplings to be equal and so requires all cross-sections to go to the same constant. While this may save the Pomeron theoretically, it removes the applicability of Gribov's Reggeon Calculus[5-7] (or any similar theoretical picture of the Pomeron as a pole plus accompanying multi-Pomeron cuts) to an energy regime that is possibly physically unattainable[2].

These theoretical problems for the Pomeron have, of course, been followed by the recent ISR measurement of a significant rise in the proton-proton total cross-section in the ISR energy range. While this has been widely interpreted as experimental evidence (to add to the theoretical evidence!) against the Pomeron as a simple pole, we now have several fits to the ISR data based on the Reggeon Calculus[8-10] which show that in fact this interpretation of the Pomeron fits very well all the features of the data. In this context it is important to note that while the Froissart bound is a very familiar s-channel constraint on models which produce asymptotically rising cross-sections, it is not at all clear that the t-channel constraints are not even stronger. Not only do the "hard" Regge cuts typical of such models have to be made consistent with the "soft-cut" requirement of two-particle unitarity[11], but also the full multiparticle equations have to be satisfied[12]. The Reggeon Calculus has the great virtue of satisfying full multiparticle t-channel unitarity. If the Pomeron can be rescued from the s-channel decoupling arguments then it is clear that a Reggeon Calculus description of it will provide a very theoretically appealing basis for understanding high-energy phenomena. We would also, of course, like to save the Pomeron as a pole for its factorization properties - particularly in inclusive processes.

The purpose of this paper is to present a self-consistent picture of the Pomeron as a pole (plus cuts) which clearly avoids the decoupling arguments. The decoupling arguments all proceed from the famous zero (which we retain) in the triple Pomeron coupling which appears in the inclusive cross-section and in the Reggeon Calculus. This zero is presumably not a theoretical requirement under all possible conditions. In particular if we allow multi-Pomeron cuts to be

highly-singular at t = 0, and do not insist that they be separable from the pole , then it may be that there is no constraint on the triple Pomeron vertex. However, in such a situation we would not expect to be able to develop a theory with any predictive power. The triple Pomeron zero must therefore be viewed as a condition on the "weakness" of the Pomeron's interaction with its cuts. This requirement is mostly clearly framed in the Reggeon Calculus. There it emerges[6,7] as the condition that the renormalized skeleton graph expansion converge at t = 0, with the Pomeron propagator receiving only mild corrections from the two-Pomeron cut. As a result the renormalized trajectory has a finite slope at t = 0. Recent experimental results[13] suggesting that the inclusive triple Pomeron vertex may indeed vanish at t = 0, provide further experimental support for a solution of this kind.

It has been shown that the s-channel arguments for the triple Pomeron zero, based on inclusive sum rules, could be invalid because of effects analogous to the AFS cancellation[14] or more general absorptive cancellations[15,16]. In these cases, however, the weak coupling condition is not imposed and complete self-consistency can not be discussed.

In this paper we shall argue that the requirement that the Pomeron self-interaction be weak should only lead to constraints on Pomeron couplings to itself and should not spread to Reggeon couplings which are simply associated with finite renormalization effects at t = 0. We make this argument explicit by invoking a particular dynamical mechanism as being responsible for the triple Pomeron zero. We generalize Bronzan's study[17] of the sum of ladder diagrams within the Reggeon Calculus by assuming that two-Pomeron iterations of an effective singular potential are responsible for the zero. We are then able to see that it is vital to take account of extra contributions to two-particle inclusive cross-sections besides the conventional Regge pole contributions. These contributions correspond to "triangle" and other "anomalous threshold" Reggeon graphs and represent a natural generalization to production processes of the Mandelstam cuts which appear in two-body processes. We show that these extra contributions lead the pole contributions for negative momentum transfer and at zero momentum transfer give the same asymptotic behaviour as the pole contributions. They may, of course, only be important at very high energies but they are vital for avoiding the decoupling arguments. We emphasize that, although we base our arguments on the Reggeon Calculus, we anticipate that the extra j-plane singularities which we find to be important are actually a general requirement of t-channel unitarity.

The outcome of our study then is that not only is the Pomeron not required to decouple from total cross-sections but also there need be <u>no inelastic decoupling</u>. However, we find that the mechanism for producing the triple Pomeron zero which we consider leads naturally to the result that the total cross-section for the
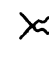
scattering of particles a and b should have the <u>universal</u> form

$$\sigma_{ab}(s) = g_a g_b \left(1 - \frac{\gamma^2}{\ln s}\right) + O\left(\frac{1}{(\ln s)^2}\right) \qquad (1.1)$$

so the combined contribution of the Pomeron pole and two-Pomeron cut factorizes and total cross-sections should become proportional before reaching their asymptotic limits. This, of course, also implies that the two-Pomeron cut will contribute negatively to all processes – the t-channel proof given in Refs. 18 applies only to processes which are elastic in the t-channel. The negative sign of the two-Pomeron cut is only indirectly related to the mechanism for producing the triple Pomeron zero and may not be essential.
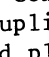
It may also be that two-Pomeron cut contributions to inclusive cross-sections (in channels where the Pomeron mass is zero) factorize in a similar way to (1.1), since this would explain the good factorization properties of such cross-sections.

Apart from normalization factors the γ that appears in (1.1) is directly given by the slope of Gribov's triple Pomeron vertex at $t = 0$. Note that γ is not directly related to the slope of the inclusive triple Pomeron vertex since the two vertices only co-incide at $t = 0$. However, we could expect the two slopes to be similar in order of magnitude. It is interesting that in this way we would recover (indirectly) the correlation between the rate of increase of the total cross-section and the large missing mass production in the inclusive cross-section, which has been obtained by several authors[19-24] using an iterative model for the Pomeron which has an effective non-zero triple Pomeron coupling. In our picture the zero mass triple Pomeron coupling must vanish, but a rapidly increasing cross-section would imply that this zero should only have any effect at very small t (where it could possibly be masked by cut contributions[25]).

Clearly the difference between (1.1) and the formulae given by Gribov[5-7], or Muzinich, Paige, Trueman and Wang[26] is the absence[*] of any "low-energy" contribution to the cut coupling (or fixed pole residue) which would be represented by a Reggeon Calculus coupling of the form ⋉ and which is normally taken to be given by the single-particle contribution of the absorption model.

$$\rightarrow \qquad (1.2)$$

The reason is that "enhancement" takes place in that this term is overwhelmed by the "bare Pomeron" contribution

---

*) It is interesting to note that the most complete fit to the ISR data is that given in Ref. 8, and in this fit the coupling N_0 (⋉) although taken to be finite at $t = 0$, is relatively small and plays a negligible role in the fit for $t \sim 0$.

$$\hspace{10cm} (1.3)$$

before two-Pomeron iteration of the potential introduces the triple Pomeron zero. This will not be the case if the triple Pomeron zero is effectively already present before two-Pomeron iteration. Formula (1.3) will not then hold since the triple Pomeron zero reduces the left-hand side to a finite quantity at t = 0. We suggest, however, that the decoupling arguments will not be avoided unless the triple Pomeron zero only appears after two-Pomeron iteration. In this case enhancement takes place and (1.1) follows.

We begin by reviewing the decoupling arguments in Section 2. We emphasize that much of the thinking behind such arguments is based on treating the Pomeron as an elementary particle. This is particularly true of the arguments presented by Gribov[2] which are partly motivated by the Reggeon Calculus treatment of Reggeons as quasi-non-relativistic particles. Gribov's original derivation of the Reggeon Calculus[5] does not, in our view, distinguish clearly enough its domain of application. As we have said, we regard the Reggeon Calculus as a very powerful means for studying the interaction of the Pomeron with its cuts and we use it to seek an explanation of the triple Pomeron zero. However, it is clearly very important to know precisely the extent to which the Pomeron can be treated as a particle.

In Section 3 then we essentially remotivate the Reggeon Calculus by first showing that the j-plane Regge cut discontinuity formulae, which control Reggeon cut contributions to the four-point function, are analogous to the unitarity equations for the scattering of non-relativistic particles. It is straightforward then to solve these equations by introducing a non-relativistic field theory Feynman graph expansion and this is, of course, Gribov's Reggeon Calculus.

We then go on to discuss Bronzan's model for the triple Pomeron vertex as a sum of Reggeon Calculus ladder graphs. Using two Pomeron unitarity extensively we discuss how a generalization of this model could give a similar mechanism for the emergence of the triple Pomeron zero in the complete theory. In this way we give generalizations of the S-matrix N/D representations of Pomeron amplitudes obtained by Bronzan[27,28] using self-consistency arguments. From the Reggeon Calculus point of view the representations we give are more realistic and it is clear how and why (1.1) emerges.

In Section 4 we continue our discussion of the "particle-like" properties of the Pomeron. We depart temporarily from the Reggeon Calculus to discuss the treatment of Pomeron scattering amplitudes, and their unitarity relations. We emphasize the importance of a proper treatment of the helicity of the Pomeron[29,30]. This is in itself sufficient to prevent the arguments given by Gribov[2] from leading to
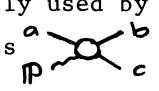
any serious decouplings. We set out in detail the circumstances under which some decouplings may be required by unitarity equations for Pomeron amplitudes,or alternatively subchannel discontinuity formulae. These decouplings refer only to certain partial-wave amplitudes and on the whole would not be physically observable. (We find that vertex signature[30] actually plays an important role in ensuring this.) The strongest result would be the vanishing of the full two Pomeron/particle vertex ∿⌣∿, but this can only be obtained by making assumptions which we suggest in Section 5 are unjustified.
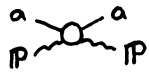
In Section 5 we discuss the interpretation of the Reggeon Calculus in the s-channel. We emphasize the qualitative nature of the arguments because of the lack of a Reggeon Calculus for production processes. To discuss inclusive processes we follow the approach of Abramovskii, Gribov and Kanchelli[31] which is based on extracting particles from the Reggeon Calculus diagrams for the four-point function. We introduce both "bare" Pomerons and Reggeons into the Calculus as multiperipheral production processes and discuss the subsequent renormalization of propagators and vertex functions. We are then able to discuss the relation between Reggeon contributions in the two-particle inclusive cross-section and the triple Pomeron vertex in terms of Reggeon renormalization of the vertex function. We then invoke the mechanism for the vanishing of the triple Pomeron vertex discussed in Section 3 to show the necessity of adding additional Reggeon contributions to the two-particle inclusive cross-section. Finally we show that these extra contributions give the leading asymptotic behaviour of the inclusive cross-section even at zero momentum transfer.

Section 6 contains a short discussion of our results, how we think they relate to other pictures of the Pomeron, and how we would hope to improve them by future research.

2. THE DECOUPLING ARGUMENTS

In this section we briefly review the various decoupling arguments as they have been presented. We shall not go over the s-channel arguments for the vanishing of the zero-mass triple Pomeron coupling $\Gamma_{ppp}(0,0,0)$ but rather accept the vanishing of this vertex as a t-channel constraint (for the reasons which we discussed in the Introduction and discuss further in the next section). Here we shall be concerned with the arguments that $\Gamma_{ppp}(0,0,0) = 0$ requires further more serious decouplings.

Gribov[2] has emphasized that further decouplings are immediately seen to be required if it is accepted that Pomeron scattering amplitudes can be treated like ordinary particle amplitudes. This is the approach originally used by Abarbanel, Ellis, Green and Zee[32]. Suppose that the Pomeron amplitudes $a\mkern-2mu\searrow\mkern-6mu\times\mkern-6mu\nearrow b$ ⫚$\swarrow\mkern-2mu\times\mkern-2mu\searrow c$ and

 satisfy the unitarity relations

(2.1)

(2.2)

Applying the Schwartz inequality to (2.1) gives
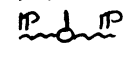
(2.3)

and using (2.) and the usual optical theorem gives

(2.4)

If we now take the mass of all Pomerons to be zero and go also to $t = 0$ then taking the high-energy limit gives

(2.5)

The powers of the asymptotic variable on the right and left-hand sides of (2.5) match up exactly at $t = 0$ and so the vanishing of $\Gamma_{ppp}(0,0,0)$ on the right-hand side also requires that the two Pomeron particle vertex vanish when both Pomerons have zero mass. This would be the original Finkelstein and Kajantie result[33].

If we now allow C to be a two particle state carrying vacuum quantum numbers then the same argument as above gives that the amplitude $\mathbb{P} \rightarrow\!\!\!\!\!\bigcirc\!\!\!\!<^{C_1}_{C_2}$ vanishes when both Pomerons have zero mass. If C_1 and C_2 carry quantum numbers then taking a further limit gives

$$\mathbb{P} \rightarrow\!\!\!\!\bigcirc\!\!\!\!< \quad \sim \quad \rightleftharpoons R \qquad (2.6)$$

where R (with $\sim\!\sim\!\sim$) represents the appropriate Reggeon exchange. If this further Regge limit commutes with the zero mass limit for the Pomerons then because of factorization we must have $\mathbb{P}\!\sim\!\!\!\bigcirc\!\!\!\sim\!R = 0$ at zero mass of the Pomeron. Brower and Weis[4] have argued that this result can be continued to the particle pole (which can be taken to be C_1) on the Reggeon trajectory to obtain the decoupling of the Pomeron from the total cross-section. This is disputed by Gribov[2], but the cancellation mechanism he argues for requires all Pomeron couplings to be the same at zero Pomeron mass and so all total cross-sections have to go to the same asymptotic limit.

To free the above argument from the need to assume unitarity relations for the Pomeron amplitudes involved, Abarbanel, Gribov and Kanchelli[34] showed that the argument could be based on subchannel discontinuity formulae. Consider the discontinuity of the five-point function in a sub-channel

$$\text{Disc } M^2 \quad \begin{array}{c} a \\ \\ e \end{array}\!\!\!\!\left(+\right)\!\!\!\!\begin{array}{c} b \\ c \\ e \end{array}\!\!\!\!\} M^2 = \sum_d \begin{array}{c} a \\ \\ e \end{array}\!\!\!\!\left(+\right)\!\!\!\!\overset{d}{\diagup}\!\!\!\!\left(-\right)\!\!\!\!\begin{array}{c} b \\ c \\ e \end{array} \qquad (2.7)$$

Applying the Schwartz inequality directly to this relation gives

$$\left| \text{Disc } M^2 \begin{array}{c} a \\ \\ e \end{array}\!\!\!\!\left(+\right)\!\!\!\!\begin{array}{c} b \\ c \\ e \end{array} \right|^2 \leq \left| \sum_d \begin{array}{c} a \\ \\ e \end{array}\!\!\!\!\left(+\right)\!\!\!\!\overset{d}{\diagup}\!\!\!\!\left(-\right)\!\!\!\!\begin{array}{c} a \\ e \\ e \end{array} \right| \left| \sum_d \begin{array}{c} b \\ \\ c \end{array}\!\!\!\!\left(+\right)\!\!\!\!\overset{d}{\diagup}\!\!\!\!\left(-\right)\!\!\!\!\begin{array}{c} b \\ c \end{array} \right| \qquad (2.8)$$

and now using the Mueller theorem together with the optical theorem gives

$$\left| \text{Disc } M^2 \begin{array}{c} a \\ \\ e \end{array}\!\!\!\!\left(+\right)\!\!\!\!\begin{array}{c} b \\ c \\ e \end{array} \right|^2 \leq \left| \text{Disc } M^2 \begin{array}{c} a \\ e \end{array}\!\!\!\!\left(\overset{+}{-}\right)\!\!\!\!\begin{array}{c} e \\ e \\ a \end{array} \right| \left| \text{Im } \begin{array}{c} b \\ \\ c \end{array}\!\!\!\!\left(+\right)\!\!\!\!\begin{array}{c} b \\ c \end{array} \right| \qquad (2.9)$$

Taking a simple Regge limit now leads directly to (2.4) and so the succeeding arguments can be followed through in exactly the same way.

The above arguments are claimed to be valid even in the presence of multi-Pomeron cuts. This should be the case for those arguments which depend only on isolating Pomeron asymptotic behaviour at the zero mass-point. A stronger argument leading to the same vanishing of the Reggeon-Pomeron-particle vertex has been given by Jones, Low, Tye, Veneziano and Young[35]. In the original presentation of this argument cuts were explicitly neglected.

Consider the sum rule which relates the one and two-particle inclusive cross-sections

$$\left(P_a + P_b - P_c\right)_\mu \quad \text{<image>} \quad = \sum_d \int d^4 P_d \ \delta^+(P_d^2 - m_d^2) \ P_{d\mu} \quad \text{<image>}$$

(2.10)

+ exclusive term

Taking the triple Pomeron limit of (2.10) and exploiting the positivity of the two-particle inclusive cross-section gives an inequality which can be graphically represented as

$$t=0 \quad \text{<image>} \quad \geq \quad \int \text{<image>}$$

(2.11)

and which can be written as[35]

$$\Gamma_{PPP}(0, t_1, t_1) \geq \int d^2 P_{d\perp} \, dy \, (1-y)^{\alpha_P(0)} \, B\left(t_1, \bar{t}, \frac{1}{1-y}, \phi\right)$$

(2.12)

If cuts are neglected then (2.11) holds for all negative t_1, since the Pomeron poles give the leading asymptotic behaviour of (2.10). If cuts are taken into account then (2.11) holds only at $t_1 = 0$.

Since $\Gamma_{PPP}(0,0,0) = 0$ it follows that

$$t=0 \quad \text{<image>} \quad = \quad B\left(0, \bar{t}, \frac{1}{1-y}, \phi\right) = 0$$

(2.13)

Finally if we assume that the limit $t_1 \to 0$ commutes with the further Regge limit $y \to 1$ in which

$$(2.14)$$

factorization requires that = 0 when the Pomeron has zero mass.

Although it is not explicit there is a sense in which the above argument attempts to treat the Pomeron like an ordinary particle. The important idea is that the three Pomeron vertex can be related to the amplitude . This follows if the Pomeron amplitude satisfies an inclusive sum rule of the form

$$(2.15)$$

3. THE t-CHANNEL PICTURE OF THE POMERON (i) AS A QUASI-NON-RELATIVISTIC PARTICLE

In the previous section we have discussed how attempts to treat a Pomeron Regge pole as an ordinary particle lie behind the various decoupling arguments. In this and the next section we shall discuss the rather complete picture of a Reggeon that emerges from t-channel unitarity, with the aim of clarifying when a Regge pole can be treated as a particle and when it can not. We shall emphasize the important distinction that must be made between the appearance of Reggeon couplings and amplitudes in cut discontinuity formulae and their appearance in the asymptotic behaviour of multiparticle amplitudes.

For the purpose of solving the Regge cut discontinuity formulae given by t-channel unitarity it is very useful to work with a Reggeon as a quasi non-relativistic particle. This is familiar from Gribov's Reggeon Calculus but it it is important to emphasize the independence of the analogy both from Gribov's original derivation of the Reggeon Calculus via the high-energy behaviour of Feynman graphs and from the existence of a perturbation solution of the cut discontinuity formulae in terms of a non-relativistic Reggeon field. To make the analogy explicit we consider first the coupled discontinuity formulae which control the contribution of the two Reggeon cut to the four-point function. The formulae can be represented pictorially by[18,36]

$$\text{disc}\ a(\jmath,t) = \quad\text{(3.1)}$$
$$\jmath = \alpha_c(t)$$

$$= \quad\text{(3.2)}$$

$$= \quad\text{(3.3)}$$

$a(j,t)$ is the Froissart-Gribov projection of the four-point function. The notation we have used in (3.1)-(3.3) naturally suggests that the Reggeon amplitudes appearing in these formulae should be identified with those of the previous section (or rather their j-plane projections). The notation also suggests that (3.2) can be obtained from (3.3) by going to integer points on two of the external Regge trajectories and that (3.1) can be obtained from (3.2) in a similar way. Unfortunately the equations are more complicated than the pictorial representation suggests.

To define ⨂ we first consider the partial-wave analysis of the six-point function corresponding to the coupling scheme of Fig. 3.1. This introduces a partial-wave amplitude $a(j,\ell_1,\ell_2,n_1,n_2,t,t_1,t_2)$ where j,ℓ_1,ℓ_2 are angular momentum labels, n_1,n_2 are helicity labels and t,t_1,t_2 are the masses of the various pairs of particles. This amplitude can be continued to complex j,ℓ_1,ℓ_2 (with ℓ_1-n_1 and ℓ_2-n_2 kept fixed). If we continue to Regge poles at $\ell_1 = n_1 = \alpha_1 \equiv \alpha(t_1)$, $\ell_2 = n_2 = \alpha_2 \equiv \alpha(t_2)$ then, after factorizing off the Reggeon/two particle vertex functions, we obtain the j-plane projection $A_{\alpha_1\alpha_2}(j,t)$ of what we shall call the full Reggeon-particle scattering amplitude (we shall enlarge upon this later).

The four-Reggeon amplitude ⨂ is defined through the partial-wave analysis of the eight-point function corresponding to the tree diagram of Fig. 3.2. Defining the partial-wave amplitude $a(j, \ell_1, \ldots, \ell_4, n_1, \ldots, n_4, t_1, \ldots, t_4)$ and then going to $\ell_1 = n_1 = \alpha(t_i)$ $i = 1, \ldots, 4$ we obtain (after factorization) the j-plane projection $A_{\alpha_1,\ldots,\alpha_4}(j,t)$ of the full four-Reggeon amplitude.

We can write (3.1) in the form

$$\text{disc}\ a(\jmath,t) = i\ \frac{\sin\frac{\pi}{2}\jmath}{2^6} \int_{\lambda(t,t_1,t_2)<0} dt_1\,dt_2\ \frac{\delta(\jmath-\alpha_1-\alpha_2+1)[-\lambda(t,t_1,t_2)]^{\frac{1}{2}}\Lambda'(\alpha_1,\alpha_2)}{t\ \sin\frac{\pi}{2}\alpha_1\ \sin\frac{\pi}{2}\alpha_2}$$
$$\times\ A_{\alpha_1\alpha_2}(\jmath^+,t)\ A_{\alpha_1\alpha_2}(\jmath^-,t)$$

$$\text{(3.4)}$$

with $\Lambda'(\alpha_1, \alpha_2) = 1 / \Gamma(2\alpha_1)\Gamma(2\alpha_2)\Gamma(2\alpha_1 + 2\alpha_2)$

We have omitted all signature labels in writing this formula since we shall assume the signatures of all Reggeons to be positive. Formula (3.4) shows that the two-Reggeon discontinuity in $a(j,t)$ can be computed solely in terms of $A_{\alpha_1\alpha_2}(j,t)$ evaluated at the nonsense-point $j = \alpha_1 + \alpha_2 - 1$. [The j^+, j^- in (3.4) refer to boundary values onto the two Reggeon cut in $A_{\alpha_1\alpha_2}(j,t)$].

It is possible to write a discontinuity formula for $A_{\alpha_1\alpha_2}(j,t)$ in terms of $A_{\alpha_1,\ldots,\alpha_4}(j,t)$ and $A_{\alpha_1\alpha_2}(j,t)$ itself and this is given in Ref. 18. However, to do this it is necessary to add $\gtrless$ labels to the definitions of both $A_{\alpha_1\alpha_2}$ and $A_{\alpha_1,\ldots,\alpha_4}$ and the formula is not a simple generalization of (3.4), although it does reduce to it at integer $\alpha_1\alpha_2$. In fact this point was illustrated in more detail in Ref. 37 where the Reggeon-particle cut was considered. Unfortunately the $\gtrless$ labels are not simply a technical complication which can be ignored. These labels have a fundamental significance in that they directly relate to the singularity structure of amplitudes allowed by the Steinmann relations.

It is possible to ignore the $\gtrless$ labels if we consider only $N_{\alpha_1\alpha_2}(j,t) \equiv$
$\equiv A_{\alpha_1\alpha_2}(j = \alpha_1 + \alpha_2 - 1, t)$, with the relevant $\gtrless$ labels averaged over. If we similarly define $N_{\alpha_1\alpha_2\alpha_3\alpha_4}(j,t)$ in terms of $A_{\alpha_1,\ldots,\alpha_4}(j,t)$ evaluated at $j = \alpha_1 + \alpha_2 - 1 = \alpha_3 + \alpha_4 - 1$ then we can write[18])

$$N_{\alpha_1\alpha_2}(j^+,t) - N_{\alpha_1\alpha_2}(j^-,t) = \frac{i \sin\frac{\pi}{2}j}{2^6} \int_{\lambda(t,t'_1,t'_2)<0} dt'_1 dt'_2 \frac{\delta(j-\alpha'_1-\alpha'_2-1)[-\lambda(t,t'_1,t'_2)]^{\frac{1}{2}}}{t \sin\frac{\pi}{2}\alpha'_1 \sin\frac{\pi}{2}\alpha'_2}$$
$$\times \Lambda'(\alpha'_1,\alpha'_2) N_{\alpha'_1\alpha'_2}(j^+,t) N_{\alpha'_1\alpha'_2\alpha_2}(j^-,t)$$

$$(3.5)$$

and also

$$N_{\alpha_1\cdots\alpha_4}(j^+,t) - N_{\alpha_1\cdots\alpha_4}(j^-,t) = \frac{i \sin\frac{\pi}{2}j}{2^6} \int_{\lambda(t,t'_1,t'_2)<0} dt''_1 dt''_2 \frac{\delta(j-\alpha''_1-\alpha''_2+1)[-\lambda(t,t''_1,t''_2)]^{\frac{1}{2}}}{t \sin\frac{\pi}{2}\alpha''_1 \sin\frac{\pi}{2}\alpha''_2}$$
$$\times \Lambda'(\alpha''_1,\alpha''_2) N_{\alpha_1\alpha_2\alpha''_1}(j^+,t) N_{\alpha''_1\alpha''_2\alpha_3\alpha_4}(j^-,t)$$

$$(3.6)$$

Equations (3.4)-(3.6) then are what we should consider to be pictorially represented by (3.1)-(3.3). Because of the nonsense conditions involved in defining the N's it is clear that (3.6) does not in general reduce to (3.5) at integer

α_3 and α_4. For example, if $\alpha_3 = \alpha_4 = 0$ in (3.6) then we must have $j = \alpha_3 + \alpha_4 - 1 = = -1$, whereas in (3.5) j is only restricted by $j = \alpha_1 + \alpha_2 - 1$. In the same way, (3.5) will not in general reduce to (3.4) at integer $\alpha_1\alpha_2$.

We emphasize that, in spite of the notation, $N_{\alpha_1\alpha_2}(j,t)$ is a function of three variables. If j and t are taken as independent variables then t_1 and t_2 are constrained by $\alpha(t_1) + \alpha(t_2) = j + 1$. Similarly $N_{\alpha_1\alpha_2\alpha_3\alpha_4}(j,t)$ is a function of four variables.

Equations (3.4)-(3.6) are a complete set of coupled equations which are sufficient if we are interested in studying the two-Reggeon cut just in $a(j,t)$. The fundamental equation is clearly (3.6) and it is from this that we shall develop the non-relativistic analogy.

We can simplify (3.6) by first extracting the threshold behaviour from $N_{\alpha_1,\ldots,\alpha_4}(j,t)$ to define

$$C_{\alpha_1\cdots\alpha_4}(j,t) = \frac{N_{\alpha_1\cdots\alpha_4}(j,t)\,t}{\lambda^{\frac{1}{2}}(t,t_1,t_2)\,\lambda^{\frac{1}{2}}(t,t_3,t_4)} \tag{3.7}$$

and then defining

$$B_{\alpha\alpha'}(j,t) = \frac{\sin\frac{\pi}{2}j\; C_{\alpha_1\alpha_2\alpha_1'\alpha_2'}\left[\lambda'(\alpha_1,\alpha_2)\,\lambda'(\alpha_1',\alpha_2')\right]^{\frac{1}{2}}}{\pi\,2^6\,\sin\frac{\pi}{2}\alpha_1\,\sin\frac{\pi}{2}\alpha_2\,\sin\frac{\pi}{2}\alpha_1'\,\sin\frac{\pi}{2}\alpha_2'} \tag{3.8}$$

(3.6) now becomes

$$B_{\alpha\alpha'}(j^+,t) - B_{\alpha\alpha'}(j^-,t) = i\pi \int_{\lambda<0} \frac{dt_1''\,dt_2''\;\delta(j-\alpha_1''-\alpha_2''+1)\;B_{\alpha\alpha''}(j^+,t)\,B_{\alpha''\alpha'}(j^-,t)}{\left[-\lambda(t,t_1'',t_2'')\right]^{\frac{1}{2}}} \tag{3.9}$$

Suppose now that we introduce two-dimensional momenta $\underline{k}$, $\underline{k}_1$, $\underline{k}_2$, $\underline{k}_1'$, $\underline{k}_2'$ such that

$$t = -\underline{k}^2 \;,\; t_1 = -\underline{k}_1^2 \;,\; t_2 = -\underline{k}_2^2 \;,\; t_1' = -\underline{k}_1'^2 \;,\; t_2' = -\underline{k}_2'^2 \tag{3.10}$$

We can impose "momentum conservation"

$$\underset{\sim}{k} = \underset{\sim}{k}_1 + \underset{\sim}{k}_2 = \underset{\sim}{k}_3 + \underset{\sim}{k}_4 \tag{3.11}$$

without constraining the t's. If we also introduce energies $\omega_i = \alpha_i(\underset{\sim}{k}_i^2) - 1$ then because of the "nonsense" conditions above we can impose "energy conservation"

$$\omega_1 + \omega_2 = \omega_1' + \omega_2' \tag{3.12}$$

Equations (3.11) and (3.12) reduce the ten momentum variables introduced in (3.10) to five. If we now regard $B_{\alpha\alpha'}(j,t)$ as a function of the $\underset{\sim}{k}$'s then it will be "invariant" under simultaneous rotation of all the $\underset{\sim}{k}$'s. This together with its remaining four-variable dependence guarantees that it can be regarded as a rotationally invariant function of four two-dimensional momenta satisfying momentum and energy conservation. That is $B(\underset{\sim}{k}_1, \ldots, \underset{\sim}{k}_2')$ can be regarded as an amplitude for the scattering of two-dimensional non-relativistic particles.

The restrictions on the region of integration in (3.9) $\lambda < 0$, and $j - \alpha_1'' - \alpha_2'' + 1 = 0$ now correspond to the condition for physical scattering and energy conservation respectively. We can actually rewrite (3.9) in the form

$$B\left(\underset{\sim}{k}_1, \ldots \underset{\sim}{k}_2'\right) - B\left(\underset{\sim}{k}_1, \ldots \underset{\sim}{k}_2'\right)^* = \frac{i\pi}{2} \int d\omega_1'' d\omega_2'' \, d^2\underset{\sim}{k}_1'' d^2\underset{\sim}{k}_2'' \, \delta\left(\omega_1 + \omega_2 - \omega_1'' - \omega_2''\right)$$

$$\times \delta^2\left(\underset{\sim}{k}_1 + \underset{\sim}{k}_2 - \underset{\sim}{k}_1'' - \underset{\sim}{k}_2''\right) \delta\left(\omega_1' - \alpha(\underset{\sim}{k}_1''^2) + 1\right) \delta\left(\omega_2' - \alpha(\underset{\sim}{k}_2''^2) + 1\right)$$

$$\times B\left(\underset{\sim}{k}_1, \ldots \underset{\sim}{k}_2''\right) B\left(\underset{\sim}{k}_1'', \ldots, \underset{\sim}{k}_2'\right)^* \tag{3.13}$$

This is now explicitly the two-particle unitarity condition (apart possible from normalization factors) for the scattering amplitude $B(\underset{\sim}{k}_1, \ldots, \underset{\sim}{k}_2)$. Higher multi-Reggeon cuts were not studied in Refs. 18 and 37 but we can infer from the work of Gribov, Pomeranchuk and Ter-Martirosyan[36] that the multi-Reggeon discontinuties of $N_{\alpha_1, \ldots, \alpha_4}(j,t)$ can be expressed in the form of multi-particle unitarity conditions for $B(\underset{\sim}{k}_1, \ldots, \underset{\sim}{k}_2')$. If this is the case then it is clear that we can study solutions of the Regge cut discontinuity formulae by studying the analogous unitarity equations for the scattering of non-relativistic particles.

This analogy is, of course, not new and is evident from Gribov's Reggeon Calculus[5-7]. The analogy has also been emphasized by Abarbanel[38] as being of importance for constructing "S-matrix" solutions of the Regge cut formulae. We have written the analogy out in detail because we think it is important to realise not only the exact sense in which the analogy is useful, but also its present

limitations. In fact we regard the Reggeon unitarity equations as the strongest motivation for the construction of a Reggeon Calculus - that is a non-relativistic Reggeon field theory. An important advantage of a Reggeon field theory solution of (3.13) over a pure "S-matrix" solution is that the "bare" propagators in the theory can be expected to have an s-channel interpretation in terms of specific production mechanisms.

There is, however, an important difference between the Reggeon discontinuity formulae and non-relativistic unitarity equations. We can illustrate this by first supposing that the single Reggeon with which we are working has intercept less than one. We have not specified the range of t for which we expect the above equations to be valid. If the intercept is less than one, however, we can take t to be negative and to lie between zero and the intersection of the Regge pole and two-Reggeon cut trajectories. In this case the trajectory function will be real, and the various Reggeon cuts will appear in the j-plane as shown in Fig. 3.3 The two-Reggeon discontinuity given by (3.6) will be $N(j + i\varepsilon, t) - N(j - i\varepsilon, t)$ (with the branch cut drawn as in Fig. 3.3). Figure 3.3 is clearly analogous to the usual energy plane picture - with the multi-Reggeon cuts simulating the multi-particle thresholds - except that the figure should be rotated through $180°$. This means that $N(j - i\varepsilon, t)$ is what should be identified with the "physical" scattering amplitude. In this case it follows from (3.6) that the "two-Reggeon cut" contributes negatively to the imaginary part of $B(k_1, k_2')$ in the "physical" boundary-value. In fact the multi-Reggeon cuts contribute with alternating signs to the imaginary part of B. This is, of course, directly related to the alternating sign of the contribution of these cuts to the total cross-section.

For $t > 0$ the integration region in (3.4)-(3.6) becomes complex if we still draw the two-Reggeon branch-cut as in Fig. 3.3. For t below the intersection of the pole and cut both the pole and cut trajectories aquire complex parts and therefore so does the integration region in (3.4)-(3.6). Therefore the pure non-relativistic analogy (apart from the sign of the cut) holds only in a very restricted t-interval. (For the Pomeron, with intercept one, this is only the point $t = 0$, which is the delicate point where all the thresholds co-incide.) Nevertheless, we anticipate that the non-relativistic analogy will be very useful outside of this range also, since this is certainly true of the field theory approach.

Before going on to field theory solutions of (3.4)-(3.6) we consider their content in terms of the nature of the singularity in $C_{\alpha_1,...,\alpha_4}$, C_{α_1,α_2}, $a(j,t)$ at $j = \alpha_c(t)$ and what can be said if these amplitudes also contain a pole at $j = \alpha(t)$. The starting-point is the deduction from (3.6) that

$$C_{\alpha_1 \cdots \alpha_4} \xrightarrow[\substack{j \to \alpha_c \\ t_1 = t_2 = t_3 = t_4 = \frac{t}{4}}]{} \frac{1}{A - \frac{\nu}{\alpha'(\frac{t}{4})} \ln(j - \alpha_c(t))} \tag{3.14}$$

where A and ν are regular at the two-Reggeon branch-point $j = \alpha_c(t)$. ν is determined by the signature and kinematic factors in (3.6) and would be one if (3.14) was written instead for $B(\underset{\sim}{k}_1, \ldots, \underset{\sim}{k}_2')$. A straightforward way to see conditions under which (3.14) can be deduced from (3.6) is as follows. Assume that the threshold behaviour shown in (3.7) is the only singular behaviour of the N's that must be considered apart from the branch-point at $j = \alpha_c(t) = 2\alpha(\frac{t}{4}) - 1$. Assume also that $C_{\alpha_1, \ldots, \alpha_4}$ can be expanded in a series of logarithms

$$C_{\alpha_1 \cdots \alpha_4} = \sum_{n=1}^{\infty} a_n \left[\ln(j - \alpha_c) \right]^{-n} \tag{3.15}$$

so that

$$C_{\alpha_1 \cdots \alpha_4}^{-1} = \sum_{n=-\infty}^{n=1} b_n \left[\ln(j - \alpha_c) \right]^{n} \tag{3.16}$$

Equation (3.16) can be substituted into both sides of (3.6) and the powers of the logarithms compared. Going to $j = \alpha_c(t)$ the integral reduces to a constant and going to $t_1 = t_2 = t_3 = t_4 = t/4$ reduces all the a_n's and b_n's to functions of t. Consequently (3.6) reduces to

$$\sum_{n=-\infty}^{n=1} b_n \left[\ln(j - \alpha_c) + i\pi \right]^{n} - \sum_{n=-\infty}^{n=1} b_n \left[\ln(j - \alpha_c) - i\pi \right]^{n} = -\frac{2\pi i \nu}{\alpha'} \tag{3.17}$$

which immediately gives

$$b_1 = \frac{\nu}{\alpha'} \quad , \quad b_0 \text{ arbitrary} \quad b_n = 0 \quad n = -1, -2, \cdots \tag{3.18}$$

Therefore, (3.14) gives an exact representation of $C_{\alpha_1, \ldots, \alpha_4}$ at $j = \alpha_c$ if $C_{\alpha_1, \ldots, \alpha_4}$ contains only logarithmically singular terms. Note that (3.15) allows for weakly singular terms in $C_{\alpha_1, \ldots, \alpha_4}$ of the form $(j - \alpha_c)^m \ln^n(j - \alpha_c)$ since these would be obtained by writing a Taylor expansion for the a_n's about $j = \alpha_c$. Also it seems difficult to envisage a more complicated singularity structure for $C_{\alpha_1, \ldots, \alpha_4}$ which is compatible with the simple constant discontinuity (that is

logarithmic discontinuity) given by the integral of (3.6) unless the N's have a complicated singular dependance on t, t_1, ..., t_4. From (3.5) and (3.4) it follows also that

$$C_{\alpha_1 \alpha_2} \quad \underset{\substack{j \to \alpha_c \\ t_1 = t_2 = \frac{t}{4}}}{\longrightarrow} \quad \frac{D}{A - \frac{\nu}{\alpha'} \ln (j - \alpha_c)} \qquad (3.19)$$

$$a(j,t) \quad \underset{j \to \alpha_c}{\longrightarrow} \quad \frac{D^2}{A - \frac{\nu}{\alpha'} \ln (j - \alpha_c)} + E \qquad (3.20)$$

where D and E are regular at $j = \alpha_c(t)$.

These equations can be derived using the analogous equations to (3.15)-(3.18).

If $a(j,t)$, $C_{\alpha_1 \alpha_2}$ and $C_{\alpha_1, \ldots, \alpha_4}$ share a Regge pole at $j = \alpha(t)$ then it clearly has to come from the vanishing of the denominator in (3.14). The vanishing of $A - \frac{\nu}{\alpha'(t/4)} \ln \left[j - 2\alpha(\frac{t}{4}) + 1 \right]$ at $j = \alpha(t)$ imposes a consistency condition on α. If we specialise to the Pomeron then the pole-cut collision occurs at $t = 0$. Bronzan[27] has shown that if A is finite at $t = 0$ then we must have $\alpha'(0) = \infty$. This leads to the vanishing of the pole residue in (3.18) so that the cross-section is given asymptotically by the two-Pomeron cut which is then forced to give a positive contribution.

To allow the two-Pomeron cut to contribute negatively to the cross-section and to obtain a self-consistent trajectory with $\alpha'(0)$ finite it is necessary to make D^2 and A singular at $t = 0$. The simplest solution is that given by Bronzan[27] in which A and D^2 share a second-order pole (which we shall call Z_0) passing through $t = 0$, $j = 1$. This pole must be second-order to avoid a square-root branch-point in (3.19). A also has a separate zero (which we shall call P_0) also passing through $t = 0$, $j = 1$. P_0 is in effect the Pomeron trajectory before its renormalization by the two-Pomeron cut. Z_0 is the triple Pomeron zero, whose origin we want to understand, as can be seen by writing (3.16)-(3.18) in the qualitative form

$$C_{\alpha_1 \cdots \alpha_4} = \frac{1}{P_0/Z_0^2 - \frac{\nu}{\alpha'} \ln (j - \alpha_c)} \qquad (3.21)$$

$$C_{\alpha_1 \alpha_2} = \frac{g/Z_0}{P_0/Z_0^2 - \frac{\nu}{\alpha'} \ln (j - \alpha_c)} \qquad (3.22)$$

$$a(j,t) = \frac{\left(\frac{a}{z_o}\right)^2}{\frac{P_o}{z_o^2} - \frac{\gamma}{\alpha'} \ln(j - \alpha_c)} \tag{3.23}$$

Clearly $C_{\alpha_1 \alpha_2}$ is finite at $j = 1$, $t = 0$ because of the cancellation between Z_0 and P_0 whereas $a(j,t) \sim \frac{1}{P_0}$ and so still has a pole.

In this solution of (3.14), (3.19), (3.20) the logarithm coming from the two-Pomeron cut is overwhelmed by Z_0^2 and it is fairly easy to see that if P_0 and Z_0 are simple linear expressions then the trajectory has only $t^2 \log t$ terms (no $\log t$ or $t \log t$) so that $\alpha'(0)$ is finite. We note, however, that E plays no role in the solution. We shall show that the Reggeon Calculus suggests a more subtle solution, involving E in a crucial way.

Gribov's original construction of a Reggeon field theory[5] was based on a direct correspondence between the perturbation theory graphs of a non-relativistic field theory and the high-energy behaviour of classes of full (four-dimensional) Feynman graphs. However, it is clear that the direct analogy between (3.6) and the non-relativistic unitarity relation (3.13) also suggests that we can construct a perturbation expansion solution of (3.6) by introducing a non-relativistic field ψ to describe the Reggeon. ψ will be a function in a fictional two-dimensional co-ordinate space, which will always be irrelevant if we are only interested in the momentum space perturbation expansion. Following Gribov and Migdal[6] we take the free Green's function $D_0(\omega,\underset{\sim}{k})$ to correspond to a linear trajectory function ($\underset{\sim}{k}$ is scaled so that $\alpha'(0) = 1$).

$$D_o(\omega, \underset{\sim}{k}) = (\omega + \underset{\sim}{k}^2)^{-1} \tag{3.24}$$

while the interaction has the general form

$$H_{int} = ir\left[\psi^+\psi^+\psi + \psi\psi\psi^+\right] + \lambda\,\psi^+\psi^+\psi\psi$$

$$+ \lambda_1\left[\psi^+\psi^+\psi^+\psi + \psi\psi\psi\psi^+\right] + \cdots \tag{3.25}$$

The couplings ir, λ, λ_1 etc. are illustrated in Fig. 3.4. They correspond to three, four ... Reggeon couplings. If it converges the renormalized perturbation expansion in terms of skeleton graphs[*] provides a series expansion solution of (3.6) (and the

---

[*] As Gribov and Migdal discuss[6], when $\omega \sim k^2 = 0$ the skeleton graph expansion may converge, whereas the complete expansion in terms of all graphs will not converge.

associated coupled multi-Reggeon equations) in powers of the renormalized vertex functions Γ_2, Γ, Γ_3, ... This then provides a powerful way of simultaneously solving the coupled equations for all the many-Reggeon amplitudes in terms of a few parameters - maybe only those needed to describe Γ_2 - this is illustrated in Fig. 3.5. The "Feynman rules" for writing down the integrals corresponding to these graphs are given by Gribov[5,6]. The amplitudes appearing in the integrals may now be "off-shell" in that we do not impose $\omega_{\mathfrak{l}} = \alpha(\underline{k}_{\mathfrak{l}}^2)$. Also in contrast to (3.13), a propagator is introduced for each internal Reggeon and the associated Reggeon energy is integrated over. Since the perturbation expansion is non-relativistic it is necessary to add diagrams which differ only by the order of emission and absorption of Reggeons.

The question then arises as to the extension of the non-relativistic analogy to (3.4) and (3.5). Gribov's original Feynman graph derivation of the Reggeon field theory applied also (and in fact primarily) to the amplitudes involved in these equations, and since the integration regions in (3.4) and (3.5) are the same as that of (3.6) it is straightforward to couple the external particles into the field theory as external sources. In principle the full renormalized amplitudes can be calculated from the integral equations coupling them to the four-Reggeon amplitude. These take the form

$$(3.26)$$

$$(3.27)$$

The amplitudes and are general two-Reggeon irreducible amplitudes. Equations (3.26) and (3.27) represent formal ways of obtaining complete solutions of (3.4) and (3.5), given , by introducing "off-shell" propagators in place of the on-shell integrations of (3.4) and (3.5), together with a "generalized potential" . For some purposes it may be sufficient to regard and as freely parametrizable within the theory and so ignore the field-theoretic expansion of these amplitudes - this will certainly involve the neglect of multi-Reggeon cuts. However, self-consistency does place some constraints on and these are naturally understood from the field theory point of view as we shall discuss. First, however, we consider the vital question of the need for and origin of, the triple-Pomeron zero.

Gribov and Migdal's original motivation[6] for the triple Pomeron zero came

from the observation that for small ω and $\underset{\sim}{k}^2$ the effective expansion parameter for the singular part of the skeleton graph expansion of Fig. 3.5 is $\Gamma_2^2 \ \omega D^3 \ \underset{\sim}{k}^2$. Therefore, if the Pomeron propagator D contains a pole with intercept one and $D \sim \omega$ as $\omega \sim \underset{\sim}{k}^2 \to 0$ the series will presumably only converge in this limit if $\Gamma_2^2 << \omega$. They then showed that no inconsistency arises if it is assumed that Γ_2 vanishes linearly, or using the notation of Fig. 3.6.

$$\Gamma_2 \left(\omega, \underset{\sim}{k} \ ; \ \sigma, \underset{\sim}{q} \right) = a \ \omega + b \ \underset{\sim}{k}^2 + c \ \underset{\sim}{q}^2 + \text{higher order terms}$$

(3.28)

"higher order terms" here includes terms of the form $q^2/\ln \omega$, $\omega/\ln \omega$ etc. The important point is that the multi-Pomeron thresholds in each of the Pomeron legs of the vertex function (as well as anomolous thresholds), which accumulate at the zero mass, zero energy point, are suppressed relative to what might be expected — for example, the two-Pomeron cut (unitarized) would be expected to produce a $1/\ln \ (\omega - \frac{1}{2}\underset{\sim}{k})$ zero of Γ_2. The suppression can take place consistently because in the full series for Γ_2 shown in Fig. 3.7 the relevant thresholds are all generated in the small "ω", small "$\underset{\sim}{k}^2$" regions (if the external ω, $\underset{\sim}{k}$, and q^2 are all small) where all the Γ_2 vertex functions involved are small by assumption. In this case the major contributions to Γ_2, in the series of Fig. 3.7, come from the finite energy regions and for (3.28) to hold it is only necessary for these to cancel to first order.

Bronzan[17] has emphasized that Gribov and Migdal provide no dynamical understanding of how their "weak-coupling" solution can be realised. He has studied the sum of Pomeron ladder diagrams shown in Fig. 3.8 as a model for Γ_2. Within this model Γ_2 satisfies the integral equation, shown graphically in Fig. 3.9

$$\Gamma_2 \left(\omega, \underset{\sim}{k} \ ; \ \sigma, \underset{\sim}{q} \right) = r - r^2 \int \frac{d^2q'}{4\pi^2} \int_{-i\infty}^{i\infty} \frac{d\sigma'}{4\pi i} \ \frac{\Gamma_2 \left(\omega, \underset{\sim}{k} \ ; \ \sigma', \underset{\sim}{q}'^2 \right)}{\left[\frac{1}{2}(\omega + \sigma') + \frac{1}{4} \left(\underset{\sim}{k} + \underset{\sim}{q}' \right)^2 \right]}$$

$$\times \frac{1}{\left[\frac{1}{2}(\omega - \sigma') + \frac{1}{4}(\underset{\sim}{k} - \underset{\sim}{q}')^2 \right]} \left[\frac{1}{\frac{1}{2}(\sigma - \sigma') + \frac{1}{4}(\underset{\sim}{q} - \underset{\sim}{q}')^2} + \frac{1}{\frac{1}{2}(\sigma' - \sigma) + \frac{1}{4}(\underset{\sim}{q} - \underset{\sim}{q}')^2} \right]$$

(3.29)

This now provides a dynamical mechanism for Γ_2 to acquire a strong zero at $\omega = \underset{\sim}{k}^2 = q^2 = 0$. All the propagators in (3.29) pinch the integration contour at this point and, unless Γ_2 has a compensating zero, this will produce an infinity

which will carry over into Γ_2. Therefore Γ_2 has to be either infinite or zero and so, if it is assumed to be finite, then it must be zero. If the "potential" represented by the propagators of the last bracket were not singular then this argument would still go through, but the zero produced by the remaining propagators would be only the inverse logarithm of the two-Pomeron cut.

Unfortunately the potential considered by Bronzan is too strong and instead of producing a simple zero in Γ_2 it produces an essential singularity. This carries over into the propagator and gives rise to an accumulation of new Regge poles at $t = 0$, $j = 1$. The original bare pole has intercept one and finite slope after renormalization but an essential singularity in the propagator would almost certainly destroy the usefulness of the Calculus, even if violation of the Froissart bound is avoided.

The full vertex will satisfy the integral equation shown in Fig. 3.10. ⟶(K)⟵ is the full one and two-Pomeron irreducible amplitude and ⟶⟨ is similarly irreducible. The Pomeron exchange terms in ⟶(K)⟵ will be softened by the presence of full triple-Pomeron vertices as shown in Fig. 3.11 and so these terms can not be considered as producing the zero in Γ_2 in the same way as in Bronzan's model. Although, of course, Γ_2 must have a zero for consistency. In fact all the potentially singular contributions to ⟶(K)⟵ will be similarly softened by the presence of softened vertices. We could assume that ⟶(K)⟵ is singular for some reason that we don't understand and that it is singular in such a way as to produce the zero of Γ_2 without the accompanying accumulation of poles found by Bronzan. This assumption would, by itself, be sufficient for the following analysis, even if it is difficult to justify in terms of particular renormalized graphs. However, it seems more likely that in the full equation of Fig. 3.10 the zero appears as a result of cancellations amongst the various terms in the iteration of ⟶(K)⟵ . This is essentially what Gribov and Migdal assumed. For this to happen it is, of course, essential for the iterations of ⟶(K)⟵ to alternate in sign and this is directly related to the negative sign of the two-Pomeron cut.

Nevertheless we would like to retain the idea, implicit in Bronzan's model, that the singular nature of the exchange of bare Pomerons (not just one necessarily) is the dynamical mechanism which produces the triple Pomeron zero. Even if ⟶(K)⟵ is not sufficiently singular we can still do this as follows. First we note that the full vertex will satisfy Bronzan's integral equation (3.29) but with a non-trivial inhomogeneous term. This is because we can always rearrange the perturbation series so that the final sum we perform is over iterations of the exchanged bare Pomerons as shown in Fig. 3.12. Of course, this rearrangement of the perturbation expansion may not be valid, but formally at least we obtain the equation shown in Fig. 3.10 with ⟶(K)⟵ given by Bronzan's kernel. The equation is not

useful however, because now the inhomogeneous term itself contains iterations of graphs very similar to $\sim\!(\!K\!)\!\sim$. For example, those with the simplest vertex insertions shown in Fig. 3.13. As a result the inhomogeneous term will itself contain an essential singularity which can cancel against that produced by the iterations of Fig. 3.12. This cancellation must take place if Γ_2 is to have only a simple zero.

We can also consider the iteration of a more complicated set of graphs. For example, a set which contains single Pomeron exchanges with only partially softened vertices. This will again give an equation of the general form shown in Fig. 3.10 which may now be useful. This will be the case if the kernel is singular in such a way as to produce a simple zero in Γ_2, provided only that the inhomogeneous term is well-behaved. The inhomogeneous term will again contain many iterations simi-lar to those we are considering but this won't matter if such iterations just pro-duce a simple zero. We, therefore, have a dynamical mechanism for producing the triple Pomeron zero if we assume that it is a consequence of an integral equation of the form of Fig. 3.10 in which the kernal $\sim\!(\!K\!)\!\sim$ is singular. $\sim\!(\!K\!)\!\sim$ may be the full set of two-Pomeron irreducible graphs, but probably it won't be. If it isn't then $\sim\!\!\prec$ will not be two Pomeron irreducible.

There are many unrenormalized graphs which will be singular in the forward direction and we shall not attempt to consider which ones could be involved. Clear-ly if the single Pomeron exchanges considered by Bronzan are involved then the hard vertex functions r must be at least partially softened by the addition of some vertex corrections. The importance of our assumption is that we will be able to consistently trace other consequences of the triple Pomeron zero, whether they refer to other Pomeron amplitudes or the decoupling arguments discussed in the previous section.

The first point to note is that the sets of one Pomeron irreducible graphs in the four Pomeron and two Pomeron/two particle amplitudes satisfy the same equations as Γ_2, but with different inhomogeneous terms, and so they must also have zeros.

Although Bronzan's model is inadequate it will be convenient for us to use it for illustrative purposes as we did in Ref. 39. The exchanged Pomerons provide an adequate graphical representation of our potential which in reality must contain a large class of graphs. As a model for the full four-Pomeron amplitude $\sim\!(\!\bigcirc\!)\!\sim$, which is consistent with Bronzan's model for Γ_2, we can take all two-Pomeron itera-tions of the Born terms

$$\rangle\!\!\!\sim\!\!\!\prec \quad , \quad \sim\!\!\!\!\perp\!\!\!\sim \quad , \quad \sim\!\!\!\!\perp\!\!\!\sim \tag{3.30}$$

so that

$$\text{(diagram)} = \text{(diagram)} + \left(\text{(diagram)} + \text{(diagram)} + \cdots \right) \tag{3.31}$$

where the one Pomeron irreducible amplitude (diagram) is given by

$$\text{(diagram)} = \text{(diagram)} + \text{(diagram)} + \text{(diagram)} + \text{(diagram)} + \cdots \tag{3.32}$$

(diagram) is given by Fig. 3.8 and

$$\text{(diagram)} = \text{(diagram)} + \text{(diagram)} + \text{(diagram)} + \cdots \tag{3.33}$$

We shall also write

$$\text{(diagram)} = \text{(diagram)} + \text{(diagram)} + \cdots \tag{3.34}$$

so (P diagram) is the full propagator in the model and, of course, (3.34) formally sums to

$$\text{(P diagram)} = \frac{1}{P_0 - \Sigma_c} \tag{3.35}$$

with P_0 being the "bare" propagator (bare of Pomeron cut renormalization that is) and Σ_c is given by the subtracted part of the set of graphs in (3.33) with the external propagators removed.

We can now use two-Pomeron unitarity to obtain representations analagous to (3.14), (3.19) and (3.20), for the various amplitudes we are considering. (diagram) satisfies two Pomeron unitarity in the form

$$\text{(diagram)} - \text{(diagram)} = \text{(diagram)} \tag{3.36}$$

(we have now crossed the Pomeron lines that are "on-shell") and so has the representation

$$\text{[diagram]} = \frac{1}{\widetilde{A} - \ln\left(\omega + \tfrac{1}{2}\underset{\sim}{k}^2\right)} \tag{3.37}$$

ν has disappeared relative to (3.14) because we are considering contributions to the scattering amplitude $B(\underset{\sim}{k}_1, \ldots, \underset{\sim}{k}_2')$ defined in (3.8) and α' has disappeared because we have scaled $\underset{\sim}{k}^2$. We are also using weak coupling in writing $\alpha(\underset{\sim}{k}^2) \sim -\underset{\sim}{k}^2 + 1$. We shall ignore the extra dependence of [diagram] on $\underset{\sim}{k}_1, \ldots, \underset{\sim}{k}_2'$ which should be introduced into (3.36) in both $\widetilde{A}$ and the numerator since this will be irrelevant for the pole-cut collision that we want to study.

The unitarity equation for [diagram] is

$$\text{[diagram]} - \text{[diagram]} = \text{[diagram]} \tag{3.38}$$

and so in analogy with (3.19) we can write

$$\text{[diagram]} = \frac{\widetilde{D}}{\widetilde{A} - \ln\left(\omega + \tfrac{1}{2}\underset{\sim}{k}^2\right)} \tag{3.39}$$

The unitarity equation for [diagram] is

$$\text{[diagram]} - \text{[diagram]} = \text{[diagram]} \tag{3.40}$$

and so comparing (3.38) with (3.19) we can write in analogy with (3.20)

$$\text{[diagram]} = \frac{\widetilde{D}^2}{\widetilde{A} - \ln\left(\omega + \tfrac{1}{2}\underset{\sim}{k}^2\right)} + \widetilde{F} \tag{3.41}$$

Since $\widetilde{F}$ represents that part of [diagram] which does not have the two Pomeron cut, the finite part of it at $\omega = \underset{\sim}{k}^2 = 0$, should have been absorbed into P_0 in the renormalization process. Therefore, we can take $\widetilde{F}$ to be zero in the following. Substituting (3.37), (3.39) and (3.41) into (3.29) we obtain

$$\text{\~{O}\~{}} = \frac{1}{\tilde{A} - \ln(\omega + \frac{1}{2}\underset{\sim}{k}^2)} + \left(\frac{\tilde{D}}{\tilde{A} - \ln(\omega + \frac{1}{2}\underset{\sim}{k}^2)}\right)^2 \frac{1}{P_o - \frac{\tilde{D}^2}{(\tilde{A} - \ln(\omega + \frac{1}{2}\underset{\sim}{k}^2))}}$$
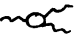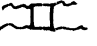
(3.42)
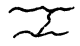
$$= \frac{1}{\dfrac{P_o \tilde{A} - \tilde{D}^2}{P_o} - \ln(\omega + \frac{1}{2}\underset{\sim}{k}^2)}$$

(3.43)
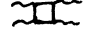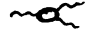
so the A of (3.14) is given by

$$A = \left(P_o \tilde{A} - \tilde{D}^2 \right) / P_o$$

(3.44)

The integral equation satisfied by $\underset{\sim}{\boxed{}}$ in Bronzan's model is analagous to (3.29) and graphically takes the form

$$\underset{\sim}{\boxed{}} = \asymp\!\asymp + \asymp\!\asymp + \underset{\sim}{\boxed{}}\!\asymp + \underset{\sim}{\boxed{}}\!\asymp$$
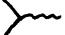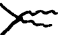
(3.45)

(Both the inhomogeneous term and the potential will be different in the full amplitude of course). The same mechanism which produces a zero in $\sim\!\!\alpha$ therefore will also produce a zero in $\underset{\sim}{\boxed{}}$. (In fact, using the variables of Fig. 3.14, it can easily be checked that $\asymp + \asymp$ is finite if the limits $\underset{\sim}{q} \to \underset{\sim}{q}''$ and $\sigma \to \sigma''$ are taken in an appropriate way, so the inhomogeneous term does not interfere with this argument even in Bronzan's model.)

If the zero of $\underset{\sim}{\boxed{}}$ is to be stronger than the logarithm of the two-Pomeron cut it must be that $\tilde{A}$ is singular at $\underset{\sim}{k}^2 = 0$. We will obtain a linear zero if we assume that $\tilde{A}$ has a simple pole, and write formally $\tilde{A} = \frac{1}{Z_o}$. (In Bronzans model $\tilde{A}$ must have an essential singularity.) From (3.39) it follows that Z_0 will similarly give Γ_2 a zero. Since the vanishings of $\underset{\sim}{\boxed{}}$ and $\sim\!\!\alpha$ are due to the same dynamical mechanism it is natural that they should have a common origin in $\tilde{A}$. From (3.44) we have

$$A = \frac{P_o - \tilde{D}^2 Z_o}{P_o Z_o}$$

(3.46)

So in contrast with (3.21) A does not have a double pole but rather has two single order poles and a single order zero coming from the vanishing of $P_0 - \tilde{D}^2 Z_0$. To see how this structure leads to consistency we go on to calculate $\quad$ and
$\quad$.

We introduce "bare" particle Pomeron couplings $\quad$ (g) and $\quad$ so that

$$\quad = \quad + \quad \qquad (3.47)$$

where in Bronzan's model

$$\quad = \quad + \quad + \quad + \, - \, - \qquad (3.48)$$

$$\quad = \quad + \quad \qquad (3.49)$$

with

$$\quad = \quad + \quad + \quad + \, - \, - \, - \qquad (3.50)$$

Therefore, we have the two-Pomeron unitarity relations

$$\quad - \quad = \quad \qquad (3.51)$$

$$\quad - \quad = \quad \qquad (3.52)$$

and so

$$\quad = \frac{\tilde{C}}{\tilde{A} - \ln\left(\omega + \tfrac{1}{2}\underline{k}^2\right)} \qquad (3.53)$$

$$\quad = \frac{\tilde{C}\,\tilde{D}}{\tilde{A} - \ln\left(\omega + \tfrac{1}{2}\underline{k}^2\right)} \qquad (3.54)$$

We can absorb $\tilde{g}$ into g and so substituting (3.39), (3.40), (3.53) and (3.54) into (3.47) gives

$$\text{(diagram)} = \frac{\tilde{C}}{\tilde{A} - \ln\left(\omega + \frac{1}{2}\underline{k}^2\right)} + \left(g + \frac{\tilde{C}\tilde{D}}{\tilde{A} - \ln\left(\omega + \frac{1}{2}\underline{k}^2\right)}\right) \times \tag{3.55}$$

$$\times \frac{\tilde{D}}{\tilde{A} - \ln\left(\omega + \frac{1}{2}\underline{k}^2\right)} \times \frac{1}{P_0 - \dfrac{\tilde{D}^2}{\tilde{A} - \ln\left(\omega + \frac{1}{2}\underline{k}^2\right)}}$$

$$= \left(\tilde{C} + g\,\tilde{D}/P_0\right) \Big/ \left(\frac{P_0\tilde{A} - \tilde{D}^2}{P_0} - \ln\left(\omega + \frac{1}{2}\underline{k}^2\right)\right) \tag{3.56}$$

Finally we take

$$\text{(diagram)} = \text{(diagram II)} + \text{(diagram)} \tag{3.57}$$

where, in Bronzan's model

$$\text{II} = \text{(diagram)} + \text{(diagram)} + \text{(diagram)} + \cdots \tag{3.58}$$

so that unitarity for II gives

$$\text{(diagram)} - \text{(diagram)} = \text{(diagram)} \tag{3.59}$$

and

$$\text{II} = \frac{\tilde{C}^2}{\tilde{A} - \ln\left(\omega + \frac{1}{2}\underline{k}^2\right)} + \tilde{E} \tag{3.60}$$

Substituting all the relevant expressions into (3.57) now gives

$$\multimap\!\!\bigcirc\!\!\multimap \ = \ \frac{\tilde{C}^2}{\tilde{A} - \ln(\omega + \tfrac{1}{2}k^2)} \ + \ \tilde{E} \ + \ \left(g + \frac{\tilde{C}\,\tilde{D}}{\tilde{A} - \ln(\omega + \tfrac{1}{2}k^2)}\right)^2 \times$$

$$\times \ \frac{1}{P_0 - \tilde{D}^2/\tilde{A} - \ln(\omega + \tfrac{1}{2}k^2)} \tag{3.61}$$

$$= \ \tilde{E} \ + \ \frac{g^2}{P_0} \ + \ \frac{\left(\tilde{C} + g\,\tilde{D}/P_0\right)^2}{\left(\dfrac{P_0\,\tilde{A} - \tilde{D}^2}{P_0}\right) - \ln(\omega + \tfrac{1}{2}k^2)} \tag{3.62}$$

If we insert $\tilde{A} = \dfrac{1}{Z_0}$ we obtain

$$\multimap\!\!\bigcirc\!\!\multimap \ = \ \tilde{E} \ + \ \frac{g^2}{P_0} \ + \ \frac{\left(\tilde{C} + g\,\tilde{D}/P_0\right)^2}{\left(\dfrac{P_0 - \tilde{D}^2 Z_0}{P_0 Z_0}\right) - \ln(\omega + \tfrac{1}{2}k^2)} \tag{3.63}$$

In this model then the D of (3.20) is given by

$$D \ = \ \tilde{C} \ + \ g\,\frac{\tilde{D}}{P_0} \tag{3.64}$$

Therefore, D^2 does have a second-order pole at $j = 1$, $t = 0$, but it originates from P_0 and not Z_0 as in (3.23). Overall the last term in (3.63) has a simple pole at $P_0 = 0$ with residue $-g^2/P_0$ and this is cancelled by the g^2/P_0 term, which appears in E in the representation (3.20). In this model it is clear that $P_0 = \omega - k^2$ represents the bare trajectory before renormalization by the two-Pomeron cut. Therefore, it is quite acceptable for E to contain a pole at $P_0 = 0$. The renormalized trajectory is given by

$$P_0 = \tilde{D}^2 Z_0 \Big/ \left(1 - Z_0 \ln(\omega + \tfrac{1}{2}k^2)\right) \tag{3.65}$$

$$= \tilde{D}^2 Z_0 + \tilde{D}^2 Z_0^2 \ln(\omega + \tfrac{1}{2}k^2) + \cdots \tag{3.66}$$

so that if Z_0 is a simple zero we have consistency with the assumed weak coupling in that the trajectory does indeed receive only a $t^2 \ln t$ modification from the two-Pomeron cut. There is a renormalization of the slope by $\tilde{D}$ but this could have been removed by giving $\tilde{F}$ a term $\tilde{D}^2/A$ in (3.41).

It is clear that the structure of (3.63) is rather different from Bronzan's solution[27] in (3.23). In fact although we have arrived at (3.62) in the context of a specific model it is clearly much more general. Equations (3.31), (3.34) – (3.44) are quite general with $\asymp$ simply defined as the one Pomeron irreducible amplitude. The following equations leading up to (3.62) can also be similarly generalized. The vital point which is not, of course, general is the tracing of the vanishing of Γ_2 to $\tilde{A}$. This is a consequence of relating the zero of Γ_2 to the iteration of a singular potential. Equation (3.63) has a fundamental significance for the following reason. Taking $t \to 0$ gives

$$\equiv\!\!\bigcirc\!\!\equiv \;\to\; \frac{g^2}{P_o} \;+\; \frac{g^2 \,\tilde{D}^2}{P_o\left(\dfrac{P_o}{Z_o} - \tilde{D}^2 - P_o \ln(\omega+\tfrac{1}{2}k^2)\right)} \tag{3.67}$$

$$\sim\; g^2\left(\frac{1}{P_o - Z_o\tilde{D}^2} \;+\; \frac{\tilde{D}^2 Z_o^2}{(P_o - Z_o\tilde{D}^2)^2}\,\ln(\omega+\tfrac{1}{2}k^2)+\cdots\right) \tag{3.68}$$

This last equation shows that the softened cut of (3.63) is "hardened" at $t = 0$. However, more importantly it shows that the factor g^2 can be factorized off from the combined cut and pole contribution. We have not considered the attachment of quantum numbers to particles. If we consider the scattering of two non-identical particles a and b it should be clear that the only quantities in (3.63) that can depend on a and b are g and $\tilde{C}$. $\tilde{D}$, P_0, Z_0 are determined only by the Pomeron or by Pomeron couplings so (3.63) will generalize to

$$\begin{array}{c} a \\ b \end{array}\!\!\bigcirc\!\!\begin{array}{c} a \\ b \end{array} \;=\; \tilde{E} + g_a g_b \;+\; \frac{\left(\tilde{C}_a + g_a \dfrac{\tilde{D}}{P_o}\right)\left(\tilde{C}_b + g_b \dfrac{\tilde{D}}{P_o}\right)}{\dfrac{P_o - \tilde{D}^2 Z_o}{P_o Z_o} \;-\; \ln(\omega+\tfrac{1}{2}k^2)} \tag{3.69}$$

and (3.68) becomes

$$\begin{array}{c} a \\ b \end{array}\!\!\bigcirc\!\!\begin{array}{c} a \\ b \end{array} \;\xrightarrow[t\to o]{}\; g_a g_b\left(\frac{1}{P_o - Z_o\tilde{D}^2} \;+\; \frac{\tilde{D}^2 Z_o^2}{P_o - Z_o\tilde{D}^2}\,\ln(\omega+\tfrac{1}{2}k^2)+\cdots\right) \tag{3.70}$$

Therefore, the combined contributions of the Pomeron pole and two-Pomeron cut to total cross-sections should always be given by the same universal function (after factorizing off the Pomeron vertices). That is all total cross-sections should become proportional before reaching their constant asymptotic limits. This also, of course, implies that the negative sign for the contribution of the two Pomeron cut will be universal and not apply only to processes that are elastic in the t-channel[18].

The above results are a consequence of assuming that the triple Pomeron zero has its origin in $\tilde{A}$. If instead $\tilde{D}$ vanished linearly, so that the triple Pomeron coupling vanished like $\omega \ln \omega$ then the $\tilde{C}_a$, $\tilde{C}_b$ terms in (3.69) would not be overwhelmed by the $g_a \tilde{D}/P_0$ and $g_b \tilde{D}/P_0$ terms. As a result the cut term would not factorize in the same way as the pole term. Also the cut would remain soft at t = 0.

It is simple to understand how our assumption that the triple Pomeron zero is generated by two-Pomeron iterations of a singular potential leads directly to (3.70). This iteration treats both the bare pole term ( ) and the bare two Pomeron/two particle coupling ( ) in identically. At t = 0 "enhancement" takes place and dominates over before iteration of the potential is considered. This is equivalent to the domination of $g\tilde{D}/P_0$ over $\tilde{C}$ in (3.64) which results in (3.68).

As we have said Gribov and Migdal[6] assumed that the triple Pomeron zero is produced by cancellations amongst graphs, but they did not envisage a dynamical mechanism of the sort we have considered. In effect they assumed that the triple Pomeron zero is already present before two Pomeron iterations are considered. To preserve the linearity of this zero after the iteration they require the four-Pomeron amplitude to also have a zero, which arises from further cancellations. In our approach this zero of the four-Pomeron amplitude is directly related to the triple Pomeron zero and we do not have to appeal to further cancellations to produce it. In terms of our N/D representations the Gribov and Migdal solution has a pole $(\frac{1}{Z_0})$ in $\tilde{A}$, but this pole is shared by $\tilde{C}$ and $\tilde{D}$. $\tilde{D}$ has a further zero which is their triple Pomeron zero. This cancels with P_0 in (3.64) so that, at t = 0, $\tilde{C}$ is not eliminated by the domination of P_0 and there is no universal factorization as in (3.70), although the cut does become hard. However, if simple cancellations (with no underlying dynamical mechanism) are responsible for the various zeros then it is very difficult to understand how the decoupling arguments of the last section can be avoided. To avoid these arguments it seems to be essential to have non-uniformities in Regge asymptotic limits and, as we show in Section 5, these are naturally provided by the singular potential we are assuming exists. For this reason we suggest that it is natural to associate factorization of the form of (3.70) with avoidance of the decoupling arguments.

Since the two-Pomeron cut contribution to the propagator is softened to the form $\omega^2 \ln \omega$ at $\underline{k}^2 = 0$, it becomes comparable with three and four Pomeron cut contributions. We should therefore have taken these cuts into account in our discussion. This is discussed by Gribov and Migdal[6,7]. Since they have the four-Pomeron coupling vanishing, the three Pomeron cut does not modify the propagator to order $\omega^2 \ln \omega$ but the four-Pomeron cut does. Therefore the four-Pomeron cut contributes to the $\ln (j - 1)$ singularity of $a(j,t)$ at $t = 0$. However, since it does this through the propagator it does it in a universal way and the factorization of (3.70) remains true.

4. THE t-CHANNEL PICTURE OF THE POMERON   (ii) AS A RELATIVISTIC PARTICLE WITH NON-INTER SPIN

Our treatment of Reggeon amplitudes in the previous section was entirely confined to nonsense amplitudes, that is "fixed-pole residue" amplitudes. We now discuss what we shall call "t-channel" results for full Reggeon scattering amplitudes. The main point we shall make is that it is vital to consider the helicity of a Reggeon as well as its spin in order to treat it to some extent as a particle. We begin by stating the results of Ref. 30 on the s-channel unitarity relation for the three particle/Reggeon amplitude $A_{\alpha(t_1)}(s,t)$ shown in Fig. 4.1.

The amplitude $A_{\alpha(t_1)}(s,t)$ is defined through a helicity-pole limit of the five-point function. To obtain an amplitude satisfying a simple s-channel unitarity relation, the Toller angle ω associated with the coupling scheme shown in Fig. 4.2 must be taken large. As a result $A_{\alpha(t_1)}$ has helicity $n = \alpha(t_1)$ in the s-channel centre of mass frame. It satisfies a two-particle unitarity relation in the s-channel in the form

$$\underset{\substack{s=4m^2}}{disc} \ A^s_{\alpha(t_1)}(s, \cos\theta) = \rho(s) \int_{-1}^{+1} d(\cos\theta') \ A^s_{\alpha(t_1)}(s, \cos\theta')$$

$$\times \left[\int_{C_R} d\nu' (\nu')^{-\alpha-1} A^-_4 - \tau_1 \int_{C_L} d\nu' (-\nu')^{-\alpha-1} A^-_4 \right]$$

$$(4.1)$$

$\cos\theta$ is the s-channel centre-of-mass scattering angle, $\rho(s)$ is the usual phase-space factor, $\nu' = e^{i\omega'}$, $A^-_4 = $ ⊐⊝⊏ and is a function of s, $\cos\theta$, $\cos\theta'$, ν'. The integrals C_R and C_L are contour integrals around the right and left-hand cuts of A^-_4, which for fixed $\cos\theta'$, appear in the ν'-plane. As shown in Ref. 30 the ν'-integration in (4.1) can be rearranged so that the equation can be written in the form

$$a \underset{c}{\overset{b}{\boxed{+}}} - a \underset{c}{\overset{b}{\boxed{-}}} = a \underset{c}{\overset{b}{\boxed{+}}} \boxed{-} + a \underset{c}{\overset{b}{\boxed{+}}} \Big| \boxed{-} \qquad (4.2)$$

where now $\underline{\underline{\quad}}$ represents the usual two-particle phase-space integration and $\underline{+}$ represents an integration over unphysical large momentum transfer regions. We shall assume that a corresponding result holds for the multi-particle discontinuities of $\boxed{\bigcirc}$ so that in general we have

$$a \underset{c}{\overset{b}{\boxed{+}}} - a \underset{c}{\overset{b}{\boxed{-}}} = \sum_d \left(\overset{d}{\boxed{+}} \boxed{\!/\!/\!} \boxed{-} + \boxed{+}\boxed{\!/\!/\!}\Big|\boxed{-} \right) \qquad (4.3)$$

where $\boxed{\!/\!/\!}$ again represents integration over unphysical large momentum transfer regions.

There are, therefore, three important features of (4.3) which are relevant if we want to use it as we used equation (2.1) in section 2. These are

i) the presence of unphysical regions in the phase-space integrations;

ii) the helicity of the Reggeon is defined in the s-channel centre of mass frame;

iii) the Reggeon/Reggeon/particle couplings which appear in $A_{\alpha(t_1)}$ are not the full couplings which appear in the double Regge limit of the five-point function.

We can argue that (i) can be neglected when considering further Regge limits if we make the dynamical assumption that large momentum transfer regions do not contribute to Regge asymptotic behaviour. To study the Regge limit taken in (2.5) it is necessary to use the t-channel amplitude $A^t_{\alpha(t_1)}(s,t)$ defined with the Reggeon having helicity $\alpha(t_1)$ in the t-channel centre-of-mass. A^s_α can be expressed in terms of t-channel amplitudes by means of the crossing-relation[30] (signature will not be important in the following argument, so as in Ref. 30 we ignore it).

$$A^s_{\alpha_1} = \frac{\sin \pi \alpha_1}{2i} \int dn \; \frac{D^{\alpha_1}_{\alpha_1, n}(c) \; a^t_>(\alpha_1, n)}{\sin \pi n \; \sin \pi (\alpha_1 - n)} + \left[n \to -n, > \to < \right] \qquad (4.4)$$

where C is the crossing transformation and $a^t_>(\alpha_1, n)$ is a partial-wave amplitude with angular momentum $\ell_1 = \alpha_1$ but with the t-channel helicity n not specifically linked to α_1. We can obtain an alternative form for (4.4) by pulling the n-contour to the left in the n-plane. For that part of A^s_α with a discontinuity in s, only

the poles at $n = \alpha_1$, $\alpha_1 - 1$, ... coming from $\sin \pi(\alpha_1 - n)$ need be considered.

In our case the Reggeon will be a Pomeron, and since we need to go to $t = 0$, we effectively need to cross a massless particle. To avoid the singularities of $D^{\alpha_1}_{\alpha_1 n}(C)$ which occur for $n < -2\alpha$, we evaluate (4.4) by moving the contour to the right in the n-plane. The important contributions now come from the $\{n \to -n\}$ term and in fact we obtain[*]

$$A^s_{\alpha_1} = \sum_{N=0}^{\infty} D^{\alpha_1}_{\alpha_1, -\alpha_1 + N}(c) \, A^t_{-\alpha_1 + N} \qquad \text{+ terms with no s discontinuity} \tag{4.5}$$

At $t_1 = 0$ when the crossing-angle becomes π we have
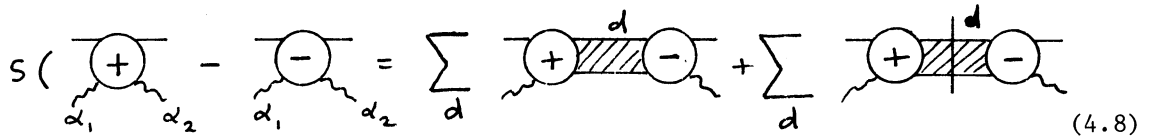
$$D^{\alpha_1}_{\alpha_1, -\alpha_1 + N}(c) = \delta_{0,N} \tag{4.6}$$

and so at $t_1 = 0$ we have the simplification that

$$\operatorname*{disc}_s A^s_{\alpha_1} = \operatorname*{disc}_s A^t_{\alpha_1} \tag{4.7}$$

since $A^t_{\alpha_1} = A^t_{-\alpha_1}$.

We also assume that the equivalent of (2.2) holds in the form

$$\tag{4.8}$$

where the Reggeons α_1, α_2 have helicities $n_1 = \alpha_1$, $n_2 = \alpha_2$ in the s-channel (note that $\pm$ refer to boundary values of in the s-channel, we do not imply that the left-hand side of (4.8) is an imaginary part). We can now apply (4.3) and (4.8) to Pomeron amplitudes to derive (2.4) as a relation between the s-channel discontinuities of s-channel Pomeron amplitudes (neglecting the contributions to (4.3) and (4.8) from unphysical regions of integration). The simple crossing relation (4.7) together with a similar relation for disc$_s$ then gives that (2.4) holds at $t = 0$ also for t-channel Pomeron amplitudes. Therefore, (2.5) follows and the two Pomeron/particle vertex involved must vanish.

At this stage point (iii) above becomes important. $A^t_{\alpha_p}$ has the Sommerfeld-Watson representation[30]

---

[*] The second term on the right-hand side of (4.5) is omitted in Ref. 30.

$$A_{\alpha_p}^t(z) = \frac{1}{2i} \int \frac{d\ell}{\sin \pi (\ell - \alpha_p)} P_\ell^{-\alpha}(z) \; \tilde{g}(\alpha_p, \ell, \alpha_p) \tag{4.9}$$

with z being the t-channel scattering angle so that

$$A_{\alpha_p(t_i)}^t \underset{|z| \to \infty}{\sim} |z|^{\alpha_p(t)} \Gamma\left(\alpha_p(t_i) - \alpha_p(t)\right) g\left(\alpha_p(t_i), \alpha_p(t), \alpha_p(t_i)\right) \beta_{\alpha_p(t)} \tag{4.10}$$

where $g[\alpha_p(t_1), \alpha_p(t), \alpha_p(t_1)]$ is simply related to the residue of the partial-wave amplitude of the five-point function, $a(\ell_1, \ell, n, t_1, t)$, at $\ell_1 = \alpha_p(t_1)$, $\ell = \alpha_p(t)$, $n = \alpha_p(t_1)$. To take the s-discontinuity of $A_{\alpha_p}(t_1)$ we first have to extract a kinematic factor $(z^2 - 1)^{-\alpha_p(t)/2}$. As a result taking the discontinuity introduces a factor $\sin \pi[\alpha_p(t) - \alpha_p(t_1)]$ which removes the pole at $\alpha_p(t_1) = \alpha_p(t)$ in (4.10) coming from the Γ-function. It then follows that (2.5) requires only that the partial-wave amplitude $\hat{g}$ satisfy

$$\hat{g}(1, 1, 1) = 0 \tag{4.11}$$

(the circumflex on g will be explained later).

This is very far from a condition on the whole two Pomeron/particle vertex as we shall discuss. First, however, we show that the alternative argument of Abarbanel, Gribov and Kanchelli[34] given in (2.7)-(2.9) leads to both (4.11) and extra conditions. The basic reason why this argument gives no serious constraint on Pomeron vertices has previously been discussed in Ref. 29.

The complete two-Reggeon/particle vertex can be written in the form (signature-particularly vertex signature τ_3, now becomes important so we include it again).

$$V_{(u)}^{\tau \tau_1} = |z|^{-\alpha} |z_1|^{-\alpha_1} \sum_{\tau_3} \int_{C_>} dn \frac{\left[(-zz_1 u)^n + \tau_3 (zz_1 u)^n\right]}{\sin \pi n} g^\tau(\alpha, \alpha_1, n)$$

$$\times \Gamma(n - \alpha) \Gamma(n - \alpha_1) \left[(-z)^{\alpha - n} + \tau_3 \tau (z)^{\alpha - n}\right]\left[(-z_1)^{\alpha_1 - n} + \tau_3 \tau_1 (z_1)^{\alpha_1 - n}\right]$$

$$+ \left\{ \begin{array}{c} > \to < \\ n \to -n \end{array} \right\} \tag{4.12}$$

If we now take α and α_1 to be Pomerons then τ and $\tau_1 = +1$. In the following we shall always evaluate (4.12) by moving the $C_>$ and $C_<$ contours to the left in the n-plane. This means that we can ignore the $\{> \to <\}$ contribution apart from its vital role in cancelling the poles at integer n in the left-half plane coming from $\sin \pi n$. Pulling back $C_>$ and dropping the contribution at infinity expresses V as a sum of two asymptotic power series in u^{-1} coming from poles of $\Gamma(n - \alpha)$ and $\Gamma(n - \alpha_1)$ respectively. As discussed in Ref. 30 taking the s discontinuity as in (2.7) ($s \equiv M^2$ in this context) removes the poles coming from $\Gamma(n - \alpha)$ by introducing a factor of $\sin \pi(n - \alpha) |z|^{\alpha-n}$ in place of $\{(-z)^{\alpha-n} + \tau_3\tau_1(z)^{\alpha-n}\}$ in (4.12). Therefore

$$\text{disc } V = \sum_{N=0}^{\infty} \frac{\left(e^{-i\pi\alpha_1} + 1\right) |u|^{-N+\alpha_1}}{\sin \pi\alpha_1} \quad \overset{\tau_3 = (-1)^N}{g} \frac{(\alpha, \alpha_1, \alpha_1, -N)}{\Gamma(N+1) \ \Gamma(N+1+\alpha_1-\alpha)} \tag{4.13}$$

We now want to consider the consequences for V of the vanishing of (4.13) at $t = t_1 = 0$. Unfortunately, the representation (4.12) is very difficult to use at this point because of kinematic singularities of the angular variables, z, z_1 and u. In fact the asymptotic expansion (4.13) will probably not converge at $t_1 = t_2 = 0$ because of this. However, the analyticity properties of the five-point function suggests that an asymptotic expansion in inverse powers of η where

$$\eta = \frac{(tt_1)^{\frac{1}{2}} \cos \omega - t - t_1 + m^2}{\lambda (t, t_1, m^2)} \tag{4.14}$$

will converge since this variable is a simple ratio of invariant variables. For t_1, $t_2 \neq 0$ the terms in (4.13) which are large or finite as $|u| \to \infty$ can be simply re-arranged into the corresponding terms in the expansion in powers of η. Therefore, the convergence of the η-expansion at $t_1 = t_2 = 0$ justifies isolating the leading terms in (4.13). A further subtlety is that the angular variables involved in defining limits on both sides of (2.4) and (2.9) are not identical and so we should compare powers of the invariant variables that are taken large. If we do this then the vertex $\hat{V}$ whose discontinuity is required to vanish at $t = t = 0$ is defined by dividing through by

$$\left| \frac{z \ \lambda^{\frac{1}{2}} (t, t_1, m^2)}{t^{\frac{1}{2}}} \right|^{\alpha} \quad \left| \frac{z_1 \ \lambda^{\frac{1}{2}} (t, t_1, m^2)}{t_1^{\frac{1}{2}}} \right|^{\alpha_1}$$

rather than by $|z|^{\alpha}|z_1|^{\alpha_1}$ as we did in (4.12). In consequence the condition that disc $\hat{V}$ vanish when $\alpha = \alpha_1 = 1$ for arbitrary finite u requires that if

$$\hat{g}^{\tau_3}(\alpha, \alpha_1, n) = \left|\frac{t^{\frac{1}{2}}}{\lambda^{\frac{1}{2}}}\right|^{\alpha} \left|\frac{t_1^{\frac{1}{2}}}{\lambda^{\frac{1}{2}}}\right|^{\alpha_1} g^{\tau_3}(\alpha, \alpha_1, n) \tag{4.15}$$

then

$$\hat{g}^{\tau_3 = (-1)^N}(1, 1, 1-N) = 0 \qquad N = 0, 1 \tag{4.16}$$
$$(t_1 = t_2 = 0)$$

(the N = 1 result here is strictly only true up to inverse powers of η). There may be further conditions besides (4.16) required to satisfy (2.9) but we can not use (4.12) to phrase them in terms of helicity amplitudes.

Since (4.16) is symmetric with respect to t and t_1 and α and α_1 it is clear that it is sufficient for the vanishing of the discontinuity of the two-Pomeron contribution to the five-point function in both sub-energy channels. However, it is important to note that this does not by itself imply the vanishing of the full two-Pomeron vertex at $t = t_1 = 0$ [40]. This can be seen immediately from (4.12).

At $\alpha_1 = \alpha_2$ the two sets of poles from $\Gamma(n - \alpha_1)$ and $\Gamma(n - \alpha_2)$ coincide and so we have to evaluate the contribution of a sequence of double poles to the integral of (4.12). If (4.16) holds then we have
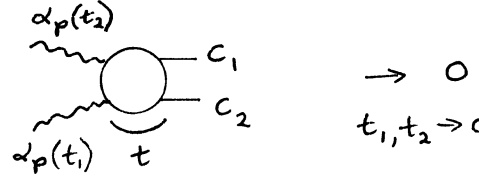
$$\hat{V}(t = t_1 = 0) = \sum_{N=0,1} \frac{|u|^{-N+1}}{[\Gamma(N+1)]^2} \left[\frac{\partial}{\partial n} \hat{g}^{\tau_3 = (-1)^N}(1, 1, n)\right]_{n = 1-N}$$
$$+ \text{ lower order terms in } \eta \tag{4.17}$$

which need not vanish.

We now consider the extension of the above arguments to involve Reggeons by using (2.6). We stress first the important point that in order to use (2.6) to derive the vanishing of a Pomeron/Reggeon/particle vertex, it is essential to make the strong assumption, that further Regge limits of Pomeron amplitudes are uniform with respect to the limit of zero masses for the Pomeron. If particle c in (4.3) is to be replaced by a two-particle state then we have to start from the unitarity relation for the four particle/Pomeron amplitude. If this is derived using the approach of Ref. 30 then the Pomeron will again have helicity $n = \alpha_p(t_1)$

in the s-channel. Using the crossing relation as above and making the same assumptions of neglecting the large momentum transfer regions will lead to the result

$$\xrightarrow{\quad} 0$$
$$t_1, t_2 \rightarrow 0 \qquad\qquad (4.18)$$

where the Pomeron with spin $\alpha_p(t_1)$ also has helicity $n_1 = \alpha_p(t_1)$ in the t-channel. The helicity n_2 of the other Pomeron will be integrated over, but for fixed n_2 the amplitude has the Sommerfeld-Watson representation.

$$A_{n_2, \alpha_p(t_1)}(t, z) = \frac{1}{2i} \int d\ell \; \frac{P_{\ell - n_2 - \alpha_1}^{(n_2 + \alpha_1, n_2 - \alpha_1)}(z) \; \tilde{g}^{\tau_3 = 1}(\alpha_2, n_2, \ell, \alpha_1, n_1 = \alpha_1)}{\sin \pi (\ell - n_2 - \alpha_p(t_1))}$$

$$(4.19)$$

τ_3 still refers to the n_1 signature, and we are ignoring all other signature and $\gtrless$ labels here. Taking the further Regge limit as in (2.6) gives the contribution of a Regge pole at $\ell = \alpha(t)$ as

$$A_{n_2, \alpha_p(t_1)} \underset{|z| \to \infty}{\sim} z^{\alpha(t_1)} \Gamma(\alpha - n_2 - \alpha_1) \; g^{\tau_3 = 1}(\alpha_2, n_2, \alpha, \alpha_1, \alpha_1) \qquad (4.20)$$

$g^{\tau_3 = 1}(\alpha_2, n_2, \alpha, \alpha_1, \alpha_1)$ is simply related to the residue to the six-point function partial-wave amplitude $a(\ell_2, n_2, \ell, \ell_1, n_1, t_2, t, t_1)$ (see Fig. 4.3) at $\ell_1 = n_1 = \alpha_1$, $\ell = \alpha$, $\ell_2 = \alpha_2$. Unitarity essentially requires[30] that g factorize in the form

$$g^{\tau_3 = 1}(\alpha_2, n_2, \alpha, \alpha_1, \alpha_1) = g(\alpha_2, n_2, \alpha) \; g^{\tau_3 = 1}(\alpha, \alpha_1, \alpha_1) \qquad (4.21)$$

where g is the analogous amplitude to that considered for the two Pomeron vertex above. Taking account of kinematic singularities as before then (4.18) will be satisfied if

$$\hat{g}^{\tau_3 = +1}(\alpha, 1, 1) = 0 \qquad (4.22)$$
$$(t_1 = 0)$$

This result is clearly similar to (4.11) and in fact if we take α to be a Pomeron is simply a stronger version of this result.

The analysis of Ref. 29 (with azimuthal angles not taken large) shows that using the approach of Abarbanel, Gribov and Kanchelli[34] simply extends (4.19) to the analogue of (4.16), that is

$$\hat{g}^{\,\hat{\tau}_3 = (-1)^N}(\alpha, 1, 1-N) = 0 \qquad N = 0, 1 \qquad (4.23)$$
$$(t_1 = 0)$$

(Again the N = 1 result is only true up to inverse powers of η.)

The correlation between the results obtained from unitarity for Reggeon amplitudes and subchannel discontinuity formulae is not surprising but it is interesting that one approach gives slightly stronger results than the other. To derive (4.16) or (4.23) from the unitarity equations for Reggeon amplitudes would require the vanishing of further triple Pomeron couplings with the helicities of two of the Pomerons differing from their spin by integer amounts. This does not seem to be required by either the Reggeon Calculus or inclusive sum rules. In this context we should perhaps note that the use of subchannel discontinuity formulae involves the assumption that these formulae continue to hold in high-energy Regge limits and this has certainly never been proved.

In general such formulae tend to hold only in a very limited region[41,42] and outside of this region the phase-space integrations are distorted by singularities of the amplitudes involved. It may be that for the helicity-pole limit isolating the external Pomeron in (2.4), no problems arise, but in the full Regge limit they do. The helicity limit is simpler than the Regge pole limit in that fewer invariants are taken large. Certainly for positive t_1 simple analytic continuation of unitarity equations to complex helicity seems to be possible[30], whereas continuation to complex angular momentum does not seem to be. If a helicity-pole limit (which is actually unphysical) of (2.9) is taken then only the weaker results of the unitarity equations for Reggeon amplitudes are obtained.

If α is a Pomeron then (4.23) requires that the two Pomeron/particle vertex amplitude have two zeros. That is

$$\hat{g}^{\,\hat{\tau}_3 = (-1)^N}(\alpha, 1, 1-N) = 0 \qquad N = 0, 1$$
$$(t_1 = 0)$$
$$\hat{g}^{\,\hat{\tau}_3 = (-1)^N}(1, \alpha_1, 1-N) = 0 \qquad N = 0, 1 \qquad (4.24)$$
$$(t = 0)$$

This would be sufficient to require that

$$\left[\frac{\partial}{\partial n} \, \hat{g}^{\tau_3 = (-1)^N}(1, 1, n) \right]_{n = 1 - N} = 0 \qquad N = 0, 1 \qquad (4.25)$$

unless $\hat{g}^{\tau_3}$ (1, 1, n) has further singularities whose origin we do not understand. In the absence of this then, it follows from (4.17) that (4.23) requires the two Pomeron/particle vertex to vanish when both Pomerons have zero mass (at least up to inverse powers of η). This is the full result of Finkelstein and Kajantie[33].

It is, of course, important to emphasize that if α is a Reggeon then (4.23) does not constrain the Pomeron coupling in the four-point function obtained by going to α = integer[29]. Suppose we consider α = 0. From (4.12) it is clear that the pole at α = 0 arises from the pinching of the n-contour by the pole at $n = \alpha$ coming from $\Gamma(n - \alpha)$ and the pole at $n = 0$ coming from $\sin \pi n$. For the residue not to vanish because of the signature factors we must have $\underline{\tau_3 = +1}$. Therefore,

$$V \underset{\alpha \to 0}{\sim} \frac{1}{\alpha} \Gamma(-\alpha_1) \frac{\left[(-z_1)^{\alpha_1} + \tau_1 (z_1)^{\alpha_1} \right]}{|z_1|^{\alpha_1}} \hat{g}^{\tau_3 = 1}(0, \alpha_1, 0) \qquad (4.26)$$

whereas only $\hat{g}^{\tau_3 = -1}(0, \alpha_1, 0)$ is constrained by (4.23). Similarly if we go to α = 2 the amplitudes involved are

$$\hat{g}^{\tau_3 = 1}(2, \alpha_1, 2), \quad \hat{g}^{\tau_3 = -1}(2, \alpha_1, 1), \quad \hat{g}^{\tau_3 = +1}(2, \alpha_1, 0) \qquad (4.27)$$

which are also unconstrained by (4.23).

So there is no inelastic decoupling of the Pomeron.

The above results can be summarized by pulling back $C_>$ to write

$$V^{\tau \tau_1} = V_1^{\tau \tau_1} |u|^{\alpha} + V_2^{\tau \tau_1} |u|^{\alpha_1} \qquad (4.28)$$

where $V_1^{\tau \tau_1}$ comes from the poles of $\Gamma(n - \alpha)$ and so, if τ = +1, contains the amplitudes

$$\left\{ \hat{g}^{\tau_3 = (-1)^{n - \alpha}}(\alpha, \alpha_1, n) \right\} \qquad (4.29)$$

while V_2^{TT1} comes from poles of $\Gamma(n - \alpha_1)$ and so contains the amplitudes
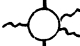
$$\left\{ g^{\tau_3 = (-1)^{n-\alpha_1}} (\alpha, \alpha_1, n) \right\} \tag{4.30}$$

V_1^{TT1} contains the particle poles on the Reggeon trajectory and so the residues of these poles contain the amplitudes (4.29). Unitarity for Pomeron amplitudes and sub-channel discontinuity formulae contrains only V_2^{TT1}, or the set of amplitudes invol-ved in (4.30).

If V^{TT1} has to vanish at $t_1 = 0$, rather than just V_2^{TT1}, then clearly the ampli-tudes of (4.29) are also constrained, and the argument of Brower and Weis[4], leading to the complete forward decoupling of the Pomeron, can be applied.

The mild results of (4.11) and (4.18) can be regarded as "t-channel" results in that they are based on unitarity equations which are derived from channels where the Pomerons involved have positive mass. They therefore make no reference to the s-channel structure of the Pomeron.

We have not discussed the full range of possible decoupling results that could be derived by extending the methods we have discussed to more complicated Pomeron amplitudes. We anticipate that for similar reasons to those we have discussed any further results also have only very mild consequences.

Finally we note that the crossing and helicity problems which we have con-sidered in this section may well complicate the derivation of an "inclusive sum rule" of the form of (2.15) from (4.8). Even if we ignore the unphysical phase-space contributions to (4.8), it is clear that a result of the form of (2.15) can only be expected to hold for amplitudes where the Pomerons have helicity $\alpha(t_1)$ in the s.channel (that is the M^2-channel for 2.15). We have already discussed crossing the two particle/two Pomeron amplitude to the t-channel and this should cause no problem at $t_1 = 0$. The amplitude appearing in (2.11) can be de-fined through a helicity-pole limit associated with the coupling scheme shown in Fig. 4.4, and so can be regarded as a t-channel helicity amplitude. However, it has a complicated singularity structure, with singularities in more than one channel. Consequently we would not expect its crossing properties to be simple in general, even if they simplify at $t_1 = 0$.

5. THE s-CHANNEL PICTURE

In this section we study how the t-channel structure discussed in Section 3 is reflected in the s-channel, and its consequences for the s-channel decoupling arguments. It will become apparent that one cannot go nearly so far with s-channel

arguments because of lack of knowledge of the structure of multi-particle amplitudes, and the possiblity of large scale cancellations. Instead of choosing a specific model of complete production amplitudes we shall attempt to re-interpret the t-channel structure in terms of the s-channel. The t-channel structure of the four-point function we take to be correctly given by the Reggeon Calculus, with the full apparatus of renormalization and the specific dynamical mechanism for achieving the triple-Pomeron zero described in Section 3. Ideally one should then formulate a Reggeon calculus of production amplitudes, along the lines suggested by Drummond[43]. Such a calculus would have of necessity to incorporate correct helicity structure, unlike the calculus for the four point function, which makes no statements about helicity. The consistency of such a scheme with s-channel unitarity would give direct information on exactly what unitarity constraints the various Reggeon-particle vertices should satisfy.

Instead one is forced to a more model-dependent standpoint. We shall adopt that of Abramovskii, Gribov and Kanchelli (AGK)[31], based on the Reggeon calculus of the four-point function. The basic propagators in the calculus will be bare Pomerons and other non-vacuum Reggeons. It is at this level that we make the s-channel interpretation: a bare Pomeron (or Reggeon) correponds to a multi-peripheral production process, that is one with a uniform distribution in rapidity space and a strong transverse momentum cut-off. This interpretation is motivated by the Feynman diagram derivation of the Reggeon calculus[5] where ladder diagrams, the prototype of all multiperipheral processes, are used as bare Reggeons. We should stress, however, that our considerations will be independent of Feynman dia-grams and use only the multiperipheral nature of the bare Reggeon. Indeed we shall ignore those special properties of the ladder diagrams which correspond to non-multiperipheral intermediate states. Such a feature is the specific mechanism of the AFS cancellation, discussed by Halliday and Sachrajda[14], which is related to the fact that ladder diagrams do not have a particularly strong transverse momentum cut-off and the AFS cancellation occurs between purely multiperipheral intermediate states and non-multiperipheral ones. In our picture the strong trans-verse momentum cut-off allows the purely multiperipheral states to cancel among themselves, on the basis of the usual analyticity arguments[44].

The bare multiperipheral Pomeron will be represented by a dashed line as in (5.1). It will have some intercept which we expect is less than one. This intercept will not however be observable (in contrast to the conclusions of Ref. 45),

$$\rangle\;\text{-----}\;\langle\;\;\approx\;\;\sum\;\;\boxed{\text{|||||||}}\qquad\qquad (5.1)$$

since in any observed purely multiperipheral event the bare mechanism is shadowed by numerous possible absorption effects, shown schematically in Fig. 5.1. This

bare Pomeron is not the bare Pomeron referred to in Section 3, which has intercept one. To generate an intercept of one, one must take into account all possible self-energy insertions in the Pomeron proagator. The analysis of Section 3 shows that in the weak-coupling solution,which we assume exists,the Pomeron cuts themselves only serve to renormalize the trajectory in a mild fashion, but not the intercept. An example of a mechanism which can increase the intercept is the insertion of Reggeon-Reggeon cuts as in (5.2), where non-vacuum Reggeons are represented by a zig-zag line. The precise form of this renormalization of the intercept is

$$(5.2)$$

model-dependent and only acquires a well-defined meaning in a given specific model. For example, in a Reggeon field theory with given bare couplings, the set of diagrams depicted above has a precise meaning. If, however, one started from the Feynman diagram derivation of the Reggeon calculus one would obtain a different result. This is because one is interested in the regions of momentum integration where there are only finite sub-energies across the Reggeon-Reggeon cuts. In this case the simple two-dimensional momentum integration around the loops breaks down, and the momentum transfers along the Reggeons depend also on the finite sub-energies[*].

These ambiguities are associated with the fact that we are taking the Reggeon calculus "off mass shell", that is, extrapolating it away from the region where the leading Reggeon singularities are generated and where it was first conjectured from the Reggeon unitarity equations as in Section 3. These ambiguities need not, however, be disadvantageous as long as one stays consistently within the same model, and they merely confirm the model-dependent and unobservable nature of the bare multiperpheral Pomeron.

It is clear that there are numerous other effects which will play a part in bringing the Pomeron intercept to one, before the inclusion of Pomeron cuts. Thus the s-channel interpretation is deeply buried inside a host of renormalization effects which vastly complicate any s-channel analysis of simple t-channel effects. One can, however, proceed a certain way in terms of largely qualitative statements and this we proceed to do.

If we consider a typical Reggeon calculus diagram constructed out of bare Pomerons and Reggeons[**], cutting the diagram in all possible ways will lead to an enormous variety of possible intermdiate states. However, there is a considerable simplification. To illustrate this consider the simple diagram of Fig. 5.2.,

---

[*] This same difficulty occurs for the renormalization of the Pomeron intercept by the finite parts of Pomeron loops (as opposed to the singular parts associated with two Pomeron cuts).

[**] Renormalization of Reggeon trajecjories will play no role in the following discussion and so we shall always refer only to renormalized physical Reggeons.

which has the Feynman diagram analogue as shown. The simplification is that cuts like C_2 are negligible, because one can then show by energy conservation that the sub-energy s' is of the same order of magnitude as the momentum transfers. This contradicts the original definition of the bare Pomeron as having all sub-energies large and all momentum transfers finite. Thus the only cuts of Fig. 5.2 we need to consider are those like C_1, where neither, just one, or both Pomerons are cut completely. Thus Fig. 5.2 contributes only to the production processes.
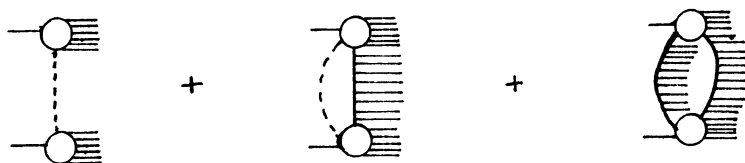
Of course, because of renormalization effects, these contributions to the exclusive processes are hopelessly buried for the model to have predictive power. On the other hand, inclusive processes can be dealt with more satisfactorily, as is shown in AGK. To discuss, for example, one-particle inclusive cross-sections in this picture one, of course, chooses one particular particle out of a possible s-channel intermediate state. This means that diagrams for the one-particle inclusive cross-section are obtained from the diagrams for the four-point function with bare Pomerons and Reggeons by attaching two particles to a cut bare Pomeron or Reggeon or cut vertex. For example Fig. 5.3 where crosses denote cut Pomerons and vertices. The reason that the model is more predictive for inclusive cross-sections is that one can now imagine the inclusion of all other diagrams contributing to the renormalization of the bare Pomerons in Fig. 5.3 and building up the diagrams of Fig. 5.4 with physical Pomerons and potentially calculable vertices, as set out in AGK.

We now discuss the s-channel decoupling arguments in terms of this picture. First we consider our specific dynamical mechanism for the triple Pomeron zero. We again use Bronzan's model[17] in an illustrative sense. We therefore consider the integral equation of (3.29), shown graphically in Fig. 3.8. If we take the discontinuity of this equation and relate it to the one-particle inclusive cross-section via the above prescription we obtain several distinct contributions on the right-hand side

$$(5.3)$$

The classification here is simply "topological" and we are grouping together terms
with the order of emission and absorption of the exchanged Pomeron reversed and
different internal Pomeron's cut. We are also implicitly assuming AGK's claim
that vertex functions are unchanged by the various ways of cutting.

The inhomegenous term (a) in (5.3) is presumably finite when all three ex-
ternal Pomerons have zero mass. Terms (c), (d) and (e) can be made finite by a
sufficiently strong zero in ~⍺ . For (b) to be finite, however, it is clear
that ~ will have to possess a zero. Therefore, it seems that a solution of
(5.3) for ~ which is finite at zero mass of the Pomerons will in fact be zero
at this point. The amplitude ~ is not sufficiently well defined within our
present scheme and so we should not immediately identify it with the amplitude
appearing in (2.11). Nevertheless, (5.3) does suggest the possibility of obtaining
a result of the form of (2.13) from t-channel arguments, and in the following we
shall make this identification.

Within the above model then the zero of ~ will be given by the sum of
diagrams

$$\sim\!\!\bigcirc\!\!\sim = \sim\!\!<\!\!\sim + \sim\!\!<\!\!\sim + \sim\!\!<\!\!\sim + \sim\!\!<\!\!\sim + \sim\!\!<\!\!\sim + \cdots$$
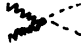
$$(5.4)$$

This sum cannot be simply associated with two-Pomeron iteration in a single channel
and so it is difficult to generalize the unitarity arguments of Section 3 to cover
this situation.

Using (5.4) we can, however, explicitly discuss how the argument of Jones
et al. can break down in going from (2.13) to (2.14). First we have to incorporate
Reggeon renormalization of vertex functions into (5.4). We have already discussed
the two Reggeon renormalization which contributes to the propagators of (5.4). If
we include a bare two Pomeron/two Reggeon coupling in our original Reggeon
calculus then there will be Reggeon renormalization of the triple Pomeron vertex
of the form

$$-\!\!\!<\!\!\sim + -\!\!\!<\!\!\sim + -\!\!\!<\!\!\sim + -\!\!\!<\!\!\sim + \cdots$$

$$(5.5)$$

As we have said, Reggeon renormalizations of this sort are simple finite effects,
which were already included in the definition of the bare triple Pomeron vertex
~ which we used in Section 3. However, the importance of (5.5) is that

after renormalization of the external Pomerons the first term leads to the con-
tribution to the two-particle inclusive cross-section considered by Jones et al.
We simply extract the single-particle intermediate state from $\rightthreetimes$ so that

$$\tag{5.6}$$

Renormalizing the external Pomeron lines therefore gives

$$\tag{5.7}$$

$$\tag{5.8}$$
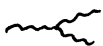
Therefore

$$\tag{5.9}$$

However, the Reggeon/Pomeron vertex $\sim\!\!\downarrow\!\!\sim$ appearing in (5.9) is not yet the
complete vertex in that we still have to add Pomeron and Reggeon renormalizations,
for example

$$\tag{5.10}$$

These renormalizations of $\sim\!\!\downarrow\!\!\sim$ simply contribute to the renormalization of
$\sim\!\!\!\!<$ via (5.8). However, it is clear that renormalizations of $\sim\!\!\!\!<$
of the form shown in Fig. 3.8, which give rise to (5.4), cannot be interpreted as
simply renormalizing $\sim\!\!\downarrow\!\!\sim$ in (5.9). Therefore these diagrams have to be
added separately. Finally then we conclude that we can write an equation of the
form (5.4) with

$$\tag{5.11}$$

where ⌇⌇⌀⌇ is the full Reggeon/Pomeron/particle vertex and so (modulo all the uncertainties of the Reggeon calculus we are using) we can identify the right-hand sides of (2.14) and (5.11). It follows then, that to produce the triple Pomeron zero, we have to add all the diagrams of (5.4) to the right-hand side of (2.14).

Addition here is, of course, in the sense that the diagrams are interpreted as Feynman diagrams within the Reggeon calculus. This essentially means adding the diagrams in a j-plane sense. The diagrams in the sum of (5.4) will give rise to a complicated singularity structure in the j-planes which control the asymptotic limits involved in (2.14), (we discuss this in more detail below but compare also Drummond's analysis[43] of ⟩⟨ and Botke's analysis[46] of ⟩⟨). Therefore, the zero of ⌇⌀⌇ is produced by adding terms which have distinguishable asymptotic behaviour in the extended limit of (2.14). It follows then that this limit cannot be uniform with respect to the zero mass Pomeron limit and this is the basic reason why the vanishing of ⌇⌇⌀⌇ cannot be deduced.

In fact we can show that (2.14) does not give the leading behaviour in the extended limit even at $\bar{t} = 0$. Consider the diagram shown in Fig. 5.5 which is part of the sum (5.4). The two particles shown have been extracted from the triple Pomeron vertex to which they are attached and the crossed Pomerons have been cut. If we again use (5.11) for the cut vertex we obtain

$$\tag{5.12}$$
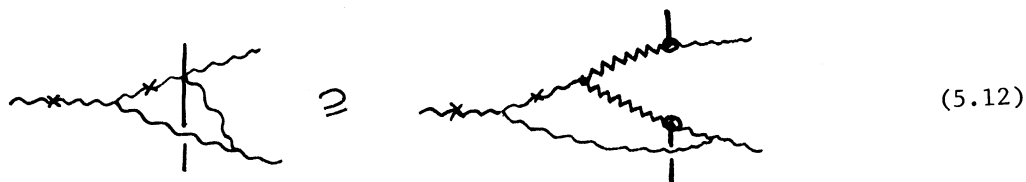
The internal cut Pomeron will not be important for our arguments and in fact a subset of the diagrams of (5.4) can be treated in the same way as (5.12) to give the general result

$$\tag{5.13}$$
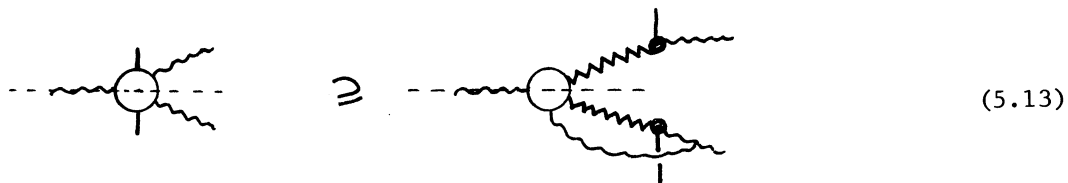
Comparing (5.13) with (2.14) is clearly analogous to comparing the five-point functions of Fig. 5.6 (a) and (b).

The diagram of Fig. 5.6 (b) will give rise to the conventional pole and cut singularities in the t and $\bar{t}$ channels shown in Fig. 5.7.

The Reggeon-Pomeron cut of Fig. 5.7 (a) is itself sufficient to ensure that the diagram of Fig. 5.6 (b) leads the pole diagram of Fig. 5.6 (a) for $\bar{t}$ negative. However, Fig. 5.6 (b) also contains the "triangle" singularity shown in Fig. 5.8, which has been studied by Drummond[43], and at $t = \bar{t} = 0$ this actually "enhances" the asymptotic behaviour given by Fig. 5.6 (b) as we now show.

This calculation can be carried out from the Feynman diagram approach (four-dimensional), in a similar manner to that of Drummond, or, more simply, in a Reggeon field theory. In the latter method we introduce Reggeon energies ω_1 and ω_2 in whose complex plane the singularities control the asymptotic behaviour in s_1 and s_2 respectively, (see Fig. 5.9 for notation). The produced particle, however, carries away a certain angular momentum and thus Reggeon energy is not conserved at the central vertex.

Ignoring momentum dependence of the various vertices, the double partial wave amplitude is, apart from constant factors

$$\int \frac{d\sigma}{2\pi i} \int d^2\underline{k} \frac{1}{(\omega_1 - \sigma + (\underline{q} - \underline{k})^2 + \Delta_R)(\sigma + \underline{k}^2)(\omega_2 - \sigma + (\underline{\bar{q}} - \underline{k})^2)(\omega_2 + \underline{\bar{q}}^2)}$$

(5.14)

where $\Delta_R = 1 - \alpha_R(0)$ and $t = -q^2$, $\bar{t} = -\bar{q}^2$. The σ-integration can be carried out to give

$$\int d^2\underline{k} \frac{1}{(\omega_1 + \underline{k}^2 + (\underline{q} - \underline{k})^2 + \Delta_R)(\omega_2 + \underline{k}^2 + (\underline{\bar{q}} - \underline{k})^2)(\omega_2 + \underline{\bar{q}}^2)}$$

(5.15)

Equation (5.15) clearly displays the various singularities discussed above. For general q and $\bar{q}$ the Reggeon-Pomeron cut in the $\bar{t}$-channel arises from the integration region $k \sim \frac{1}{2} \bar{q}$, and the Pomeron-Pomeron cut in the t-channel from $k \sim \frac{1}{2} q$. The triangle singularity arises when these collide near $q \sim \bar{q}$. This is in fact a singularity in η ($= s_1 s_2 | s$) by virtue of the relation $\eta = m^2 + (q - \bar{q})^2$, and it occurs on the boundary of the physical region in η. One can show that the η for the internal Pomeron-Reggeon-particle vertex is equal to the η defined by the external variables of the whole diagram, and so we expect no other new singularities in η apart from the triangle described above. When $q = \bar{q} = 0$ the singularities all enhance each other and the asymptotic behaviour is given by (ignoring signature factors)

$$\int \frac{d\omega_1}{2\pi i} \int \frac{d\omega_2}{2\pi i} \; s_1^{\omega_1+1} \, s_2^{\omega_2+1} \int_0^\infty dx \; \frac{1}{(\omega_1 + x + \Delta_R)(\omega_2 + x)\,\omega_2} \qquad (5.16)$$

$$= s_1^{\alpha_R(0)} \, s_2 \int_0^\infty dx \; \frac{e^{-\xi_1 x}}{x} \left[\, 1 - e^{-\xi_2 x} \,\right] \qquad (5.17)$$

where $\xi_1 = \ln s_1$, $\xi_2 = \ln s_2$.

When ξ_1 and ξ_2 are large and of the same order of magnitude the integral in (5.17) is just a finite number, as can be shown by scaling $x = x'/\xi_1$. Thus the contribution of Fig. 5.6 (b) is of the same order as the pure pole contribution.

We have identified just one contribution in the sum of (5.4) that is important in the extended limit of (2.14) but there will be others. Also we have stayed within Bronzan's model in this section in order to be able to discuss specific Reggeon calculus diagrams, and within this model it is consistent to ignore the momentum dependence of the vertices in Fig. 5.9. A complicated potential of the form that we suggested in Section 3 is more difficult to discuss, but the essential feature is contained in the above discussion. The enhancement of the Reggeon-Pomeron cut in Fig. 5.9 can be regarded as due to the singularity of the central Pomeron propagator (produced at the Reggeon/particle/Pomeron vertex). This is the Pomeron that would be replaced by the full singular potential in the complete amplitude. Clearly enhancement will be produced by the singular potential in a similar way.

For general $\bar{t}$ the Pomeron amplitude obtained from Fig. 5.9 (see Fig. 5.10) will be singular at $t = 0$ because of the collision of the two-Pomeron cut (in the t-channel) with the pole. Again a singularity at $t = 0$ of this sort will also occur if the central Pomeron is replaced by our general singular potential. This is the non-uniformity of the $\bar{t}$ Regge expansion which we referred to earlier as being the basic cause of the breakdown of the decoupling arguments.

If the Reggeon calculus does extend to production amplitudes in a straightforward way, then we might expect the further vanishings of Pomeron vertices described in Section 4 to be attributable to the same dynamical mechanism. In this case we might expect the vanishing of the two Pomeron/particle vertex amplitude to arise from a series of diagrams of the form (again using Pomeron exchange for our singular potential).

$$\text{(5.18)}$$

Similarly the vanishing of the two-particle/two Pomeron amplitude as in (4.18) should result from a sum of the form

$$\text{(5.19)}$$

Consequently we would not expect the extended limit of (2.6) to be uniform with respect to the zero mass Pomeron limit.

In general then our understanding of zero mass Pomeron zeros is such that we do not expect any of the results based on taking further asymptotic limits of amplitudes that vanish to go through. This rules out any results on Reggeon couplings. This is in accord with our picture of the triple Pomeron zero being associated simply with Pomeron self-renormalization problems. Reggeon contributions are associated with finite renormalization effects, which should not be constrained by the weak coupling of the Pomeron.

As we discussed in Section 3, Gribov and Migdal have the triple Pomeron zero appearing before two Pomeron cut iterations are considered. This would clearly impose more serious decoupling constraints. The sums of diagrams we have considered could no longer be appealed to. Therefore, the extended limit arguments, particularly that of (2.14) would presumably go through. This is why we suggested in Section 3 that our association of the triple Pomeron zero with two-Pomeron iteration of a singular potential is vital for the avoidance of the decoupling arguments.

6. DISCUSSION

Our aim in this paper has been to present a general framework within which it is clear that a consistent picture of the conventional Pomeron as a pole plus cuts can be obtained. We have emphasized the qualitative nature of our discussion in Section 5. This has partly been because of our desire to present an over-all picture, but more importantly because of the difficulty of performing s-channel calculations that are sufficiently realistic. We have based our arguments on the Reggeon calculus since this is the only practical way of obtaining an s-channel picture that is consistent with t-channel unitarity. However, even the Reggeon calculus is not yet applicable to production amplitudes. Eventually we may hope to be able to give a complete description of multi-particle partial-wave amplitudes in terms of Reggeon field theory diagrams. This would enable us to give a more precise version of the discussion in Section 5.

In general terms what we are saying is that absorption effects in multi-particle amplitudes are both complicated and very important theoretically. Their theoretical importance is not, as yet, something we can estimate quantitatively. We can only say that they are important for the decoupling arguments, but may be unimportant phenomenologically. In principle it may be possible to discuss these effects independently of the Reggeon calculus. General discontinuity formulae for mult-Reggeon singularities analogous to the two-Reggeon cut discontinuity formulae can presumably be obtained from multi-particle t-channel unitarity. We could then envisage parametrizing the amplitudes appearing in these formulae within some sort of "S-matrix" approach. However, it seems likely that the Reggeon calculus approach will be more fruitful. Also the extension of the calculus to both inclusive and exclusive production processes may well sharpen its predictive power.

There are many problems in extending the Reggeon calculus. The results of Section 4 and of Ref. 30 make it clear that the helicity of a Reggeon must play an essential role in any treatment of multi-particle amplitudes and this has not yet appeared in the calculus. The subtlety of the unitarity relations for Reggeon amplitudes discussed in Section 4 and Ref. 30 suggests that the vertex functions of the Reggeon calculus cannot be cut freely in taking discontinuities as suggested by Abramovskii, Gribov and Kanchelli[31] and implicitly assumed by us in Section 5. Therefore, even the understanding that this assumption provides of the emergence through the s-channel of the negative sign for the two-Pomeron cut represents an over-simplification (which probably only holds exactly for the simplest Feynman diagrams[14]).

Nevertheless, it is clear that a self-consistent description of diffraction scattering,in all its aspects,must be able to incorporate both s-channel absorption effects and full multi-particle t-channel unitarity systematically. This is what we feel can be done in principle within the Reggeon calculus,and what is missing from other schemes,which essentially ignore t-channel unitarity and either postpone absorption to satisfy the Froissart bound at ultrahigh energies[19,20] or else assume that it is negligible and that consistency can be achieved with a Pomeron intercept less than one and a positive sign two-Pomeron cut[21-24]. The importance of a correct treatment of absorption effects has recently been emphasized by Blankenbecler, Fulco and Sugar[15]. In particular Blankenbecler[16] has shown that the rise of the proton-proton total cross-section at ISR energies cannot be simply attributed to large missing mass production via the triple Pomeron and that the self-consistency of the Pomeron must be considered. From this point of view our indirect association of large missing mass production with the rising cross-section,through (1.1),seems more satisfactory.

REFERENCES

1)   F.E. Low, Proc. XVI Intern. Conf. on High-Energy Physics (1972).

2)   V.N. Gribov, Proc. XVI Intern. Conf. on High-Energy Physics (1972).

3)   For an up to date review of these arguments see, R.C. Brower and
     J.H. Weis - "Pomeron Couplings" Cal. Tech. Washington Preprint (1973).

4)   R.C. Brower and J.H. Weis, Phys. Letters $\underline{41}$ B, 631 (1972).

5)   V.N. Gribov, Zh. Eksp. Teor. Fiz. $\underline{53}$, 654 (1967) [Sov. Phys. JETP $\underline{26}$, 414
     (1968)].

6)   V.N. Gribov and A.A. Migdal, Yad. Fiz. $\underline{8}$, 1002 (1968) [Soviet J. of Nuclear
     Phys. $\underline{8}$, 583 (1969)].

7)   V.N. Gribov and A.A. Migdal, Yad. Fiz. $\underline{8}$, 1213 (1968) [Soviet J. of Nuclear
     Phys. $\underline{8}$, 703 (1969)]

8)   C. Pajares and D. Schiff, preprint LPTHE 73/13 (1973).

9)   J.N. Ng and U.P. Sukhatme, preprints RLO 1388-645, RLO 1388-652 (1973).

10) N.S. Craigie and G. Preparata, preprint DESY 73-12 (1973).

11) J.B. Bronzan and C.E. Jones, Phys. Rev. $\underline{160}$, 1494 (1967).

12) A.R. White, Nucl. Phys. $\underline{B39}$, 461 (1972).

13) S. Childress, P. Franzini, J. Lee-Franzini, R. McCarthy and R. Schamberger,
     Jr., Columbia-Stony Brook preprints (1973).

14) I.G. Halliday and C.T. Sachrajda, Imperial College Preprint, ICTP 73/18
     (1973).

15) R. Blankenbecler, J.R. Fulco and R.L. Sugar, SLAC preprint (1973).

16) R. Blankenbecler, SLAC preprint (1973).

17) J.B. Bronzan, Phys. Rev. $\underline{D7}$, 480 (1972).

18) A.R. White, Nuclear Phys. $\underline{B50}$, 130 (1972).

19) D. Amati, L. Caneschi and M. Ciafaloni, CERN preprint TH 1676 (1973).

20) J. Finkelstein, Columbia preprint CO 2271.17 (1973).

21) W.R. Frazer, D.R. Snider, Phys. Letters $\underline{45}$ B, 136 (1973).
     W.R. Frazer, D.R. Snider and C.I. Tan, preprint UCSO, IOP 10-127 (1973).

22) A. Capella, M.S. Chen, M. Kugler and R.D. Peccei, preprint SLAC PUB 1241,
     ITP-434 (1973).

23) G.F. Chew, preprint LBL-1556 (1973).

24) M. Bishari and J. Koplik, Phys. Letters $\underline{44}$ B, 175 (1973).

25) J.L. Cardy, Nuclear Phys. $\underline{B56}$, 605 (1973).

26) I.J. Muzinich, F.E. Paige, T.L. Trueman and L.L. Wang, Phys. Rev. D6, 1048 (1972).

27) J.B. Bronzan, Phys. Rev. D4, 1097 (1971).

28) J.B. Bronzan, Phys. Rev. D6, 1130 (1972).

29) I.O. Moen and A.R. White, Phys. Letters 42 B, 75 (1972).

30) A.R. White, CERN preprint 1657 (1973).

31) V. Abramovskii, V.N. Gribov and O.V. Kanchelli, Proc. XVI Intern. Conf. on High-Energy Physics.

32) H.D.I. Abarbanel, S.D. Ellis, M.B. Green and A. Zee (unpublished).

33) J. Finkelstein and K. Kajantie, Phys. Letters 26 B, 305 (1968), Nuovo Cimento 56 A, 659 (1968).

34) H.D.I. Abarbanel, V.N. Gribov and O.V. Kanchelli (unpublished).

35) C.E. Jones, F.E. Low, S.-H. Tye, G. Veneziano and J.E. Young, Phys. Rev. D6, 1033 (1972).

36) V.N. Gribov, I. Ya Pomeranchuk and K.A. Ter-Martirosyan, Phys. Rev. 139 B, 184 (1965).

37) A.R. White, Nuclear Phys. B50, 93 (1972).

38) H.D.I. Abarbanel, Phys. Rev. D6, 2788 (1972).

39) J.L. Cardy and A.R. White, CERN preprint 1726 (1973). This paper essentially contains a summary of the main results of the present paper.

40) M.B. Green - private communication.

41) A.R. White, Nuovo Cimento 59 A, 545 (1969).

42) P.V. Landshoff, D.I. Olive and J.C. Polkinghorne, J. Math. Phys. 7, 1593 (1966).

43) I.T. Drummond, Phys. Rev. 176, 2003 (1968).

44) H.J. Rothe, Phys. Rev. 159, 1471 (1967).

45) K.A. Ter-Martirosyan, Phys. Letters 44 B (1973).

46) J.C. Botke, Nuclear Phys. B42, 589 (1972).

Figure captions

Fig. 3.1   :   Tree diagram for the six-point function.

Fig. 3.2   :   Tree diagram for the eight-point function.

Fig. 3.3   :   The j-plane.

Fig. 3.4   :   Bare couplings in the Reggeon Calculus.

Fig. 3.5   :   Skeleton graph expansion for the four-Pomeron amplitude.

Fig. 3.6   :   Variables for the three-Pomeron vertex.

Fig. 3.7   :   Full skeleton graph expansion for the triple-Pomeron vertex.

Fig. 3.8   :   Bronzan's model for the triple-Pomeron vertex.

Fig. 3.9   :   Bronzan's integral equation for the triple-Pomeron vertex.

Fig. 3.10 :   Integral equation for the full vertex.

Fig. 3.11 :   Pole terms in the full potential.

Fig. 3.12 :   Rearrangement of the perturbation expansion of the triple-Pomeron vertex.

Fig. 3.13 :   Iteration of pole terms with vertex insertions.

Fig. 3.14 :   Variables for the four-Pomeron amplitude.

Fig. 4.1   :   A three particle/Reggeon amplitude.

Fig. 4.2   :   s-channel coupling scheme.

Fig. 4.3   :   Tree diagram for the six-point function.

Fig. 5.1   :   Absorption effects.

Fig. 5.2   :   Cuts through the bare two-Pomeron diagram.

Fig. 5.3   :   Bare Pomeron diagrams for the one-particle inclusive cross-section.

Fig. 5.4   :   Renormalized diagrams.

Fig. 5.5   :   Extraction of particles from an internal triple-Pomeron vertex.

Fig. 3.1

Fig. 3.2

Fig. 3.3

$i\tau$, λ , λ_1

Fig. 3.4

Fig. 3.5

$\omega, \underset{\sim}{k}$ ⟶ $\frac{1}{2}(\omega+\sigma), \frac{1}{2}(\underset{\sim}{k}+q)$

$\frac{1}{2}(\omega-\sigma), \frac{1}{2}(\underset{\sim}{k}-q)$
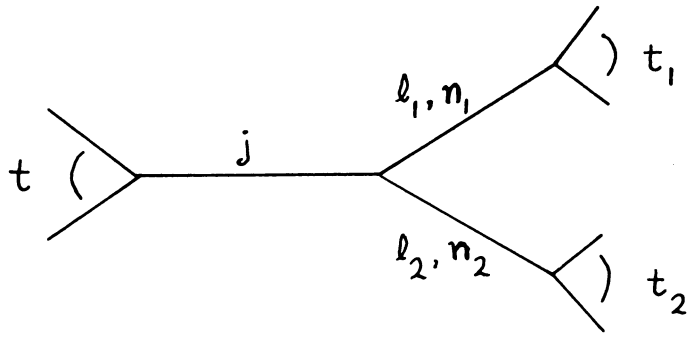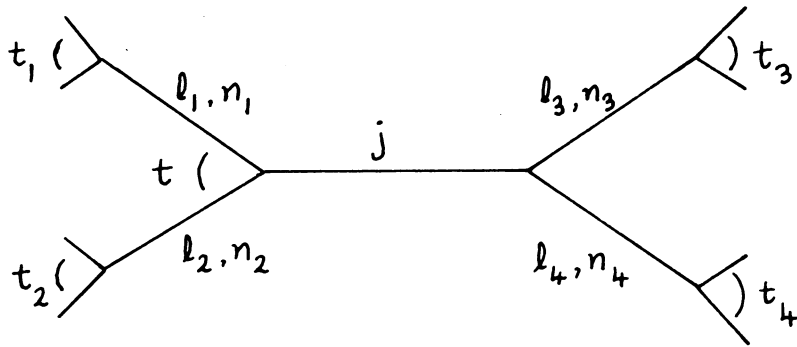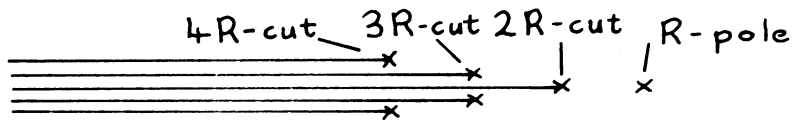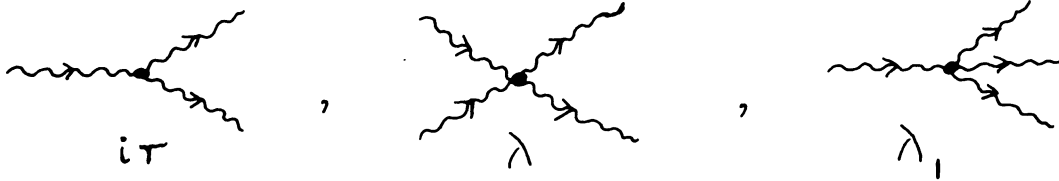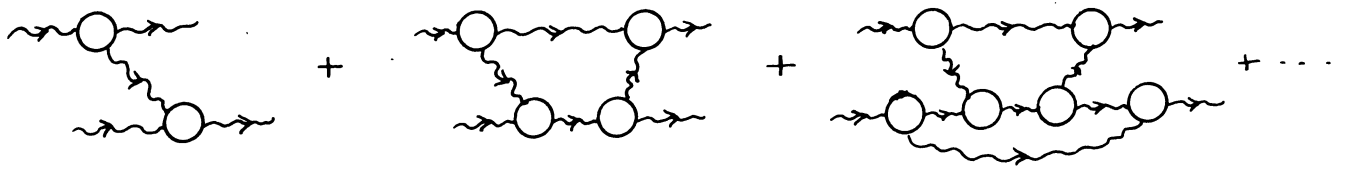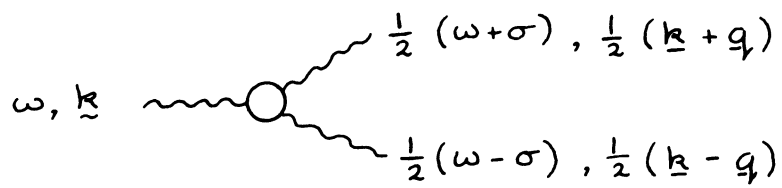
Fig. 3.6
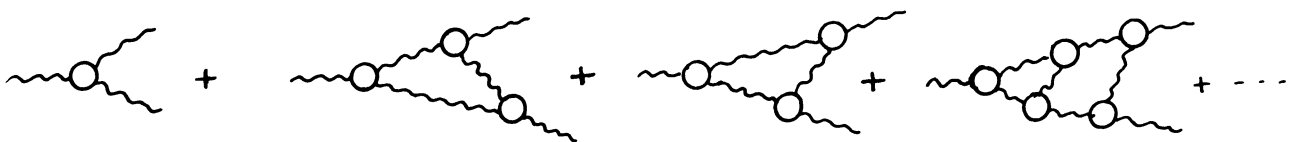
Fig. 3.7
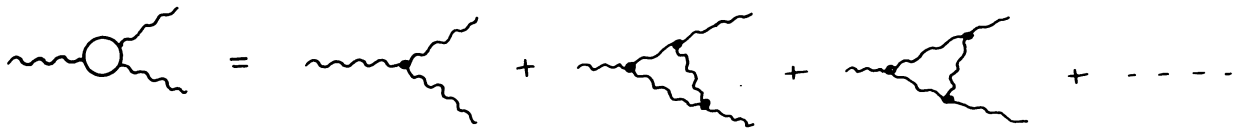
Fig. 3.8
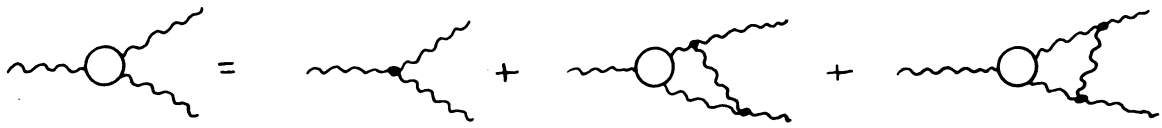
Fig. 3.9
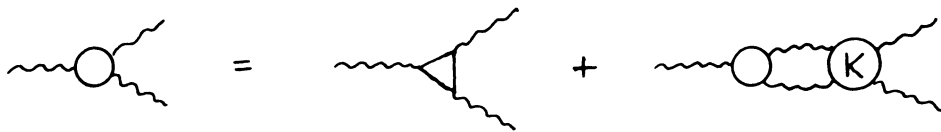
Fig. 3.10

Fig. 3.11

Fig. 3.12

Fig. 3.13

$$\tfrac{1}{2}(\omega+\sigma''), \tfrac{1}{2}(\underline{k}+\underline{q}'') \qquad \tfrac{1}{2}(\omega+\sigma), \tfrac{1}{2}(\underline{k}+\underline{q})$$

$$\tfrac{1}{2}(\omega-\sigma''), \tfrac{1}{2}(\underline{k}-\underline{q}'') \qquad \tfrac{1}{2}(\omega-\sigma), \tfrac{1}{2}(\underline{k}-\underline{q})$$
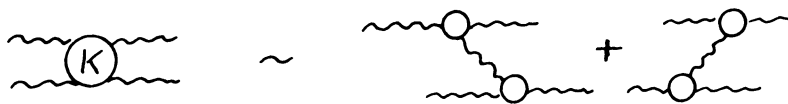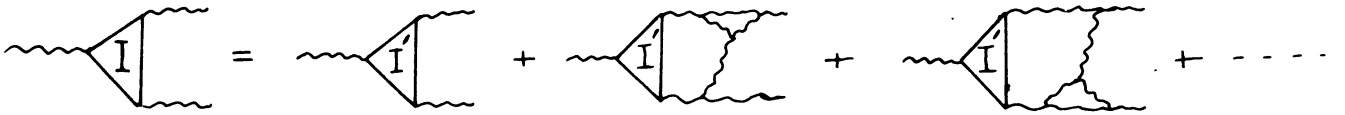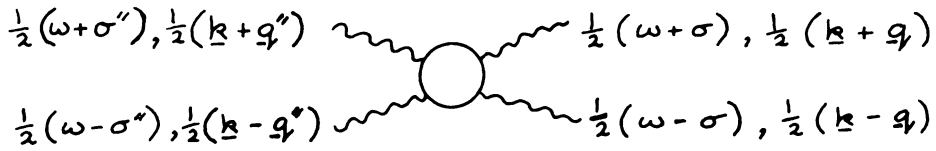
Fig. 3.14
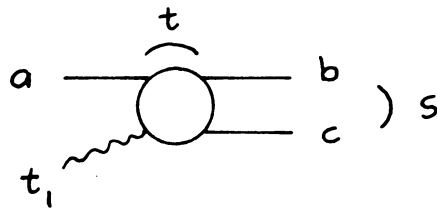
Fig. 4.1
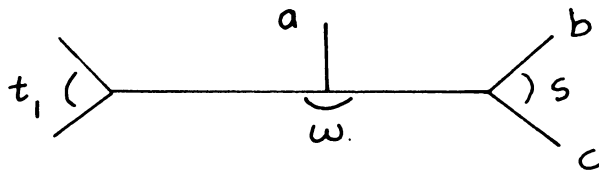
Fig. 4.2

Fig. 4.3

Fig. 5.1

Fig. 5.2

(a)   (b)
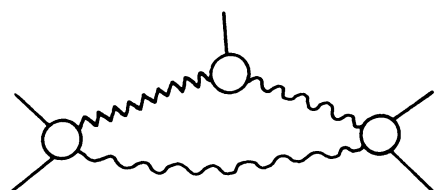
Fig. 5.3

(a)   (b)
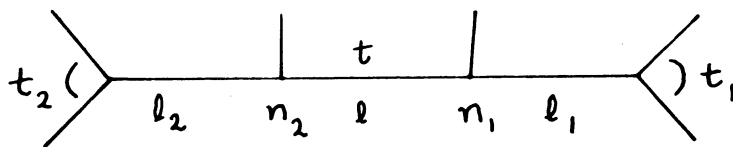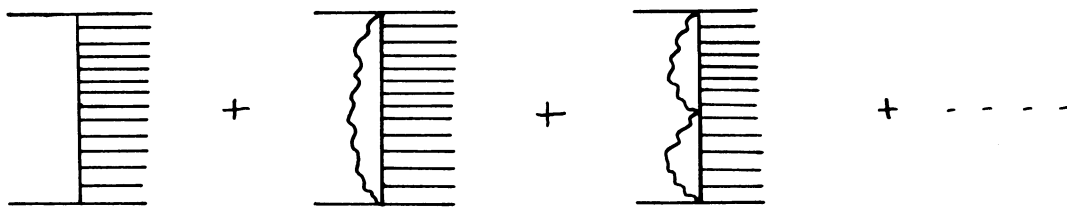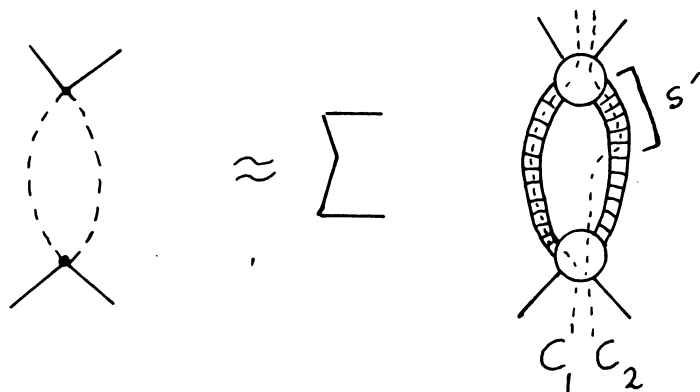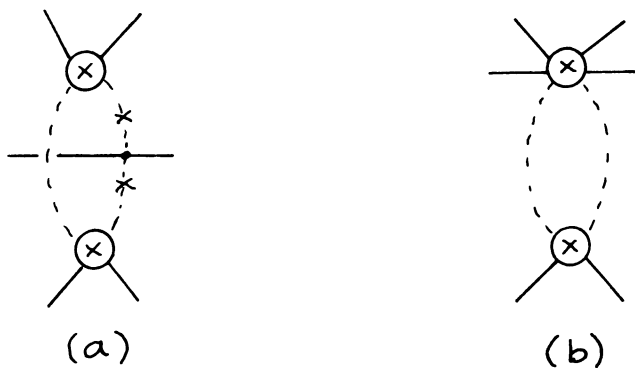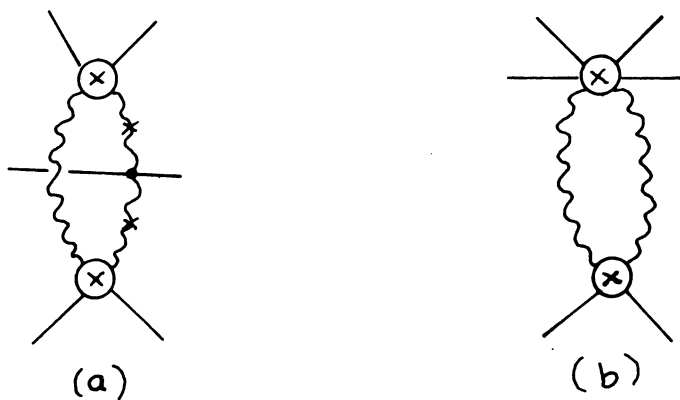
Fig. 5.4
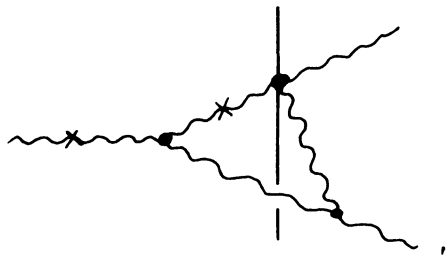
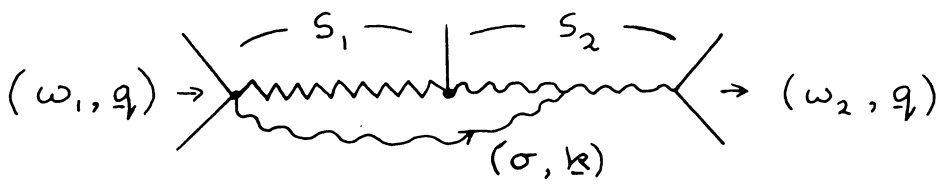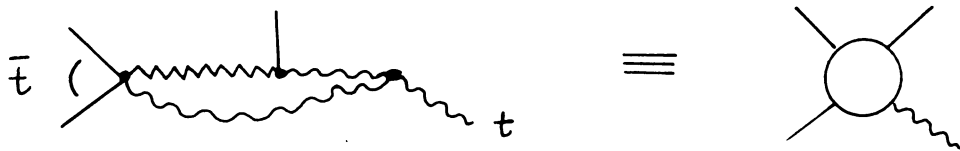Fig. 5.5
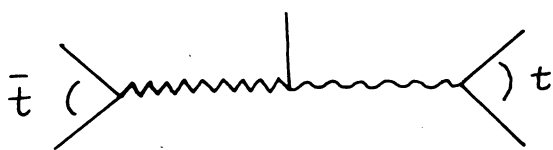
(a)
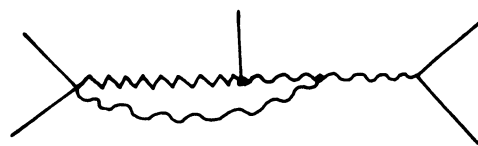
(b)

Fig . 5. 6
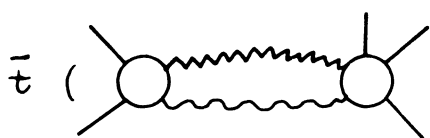
(a)
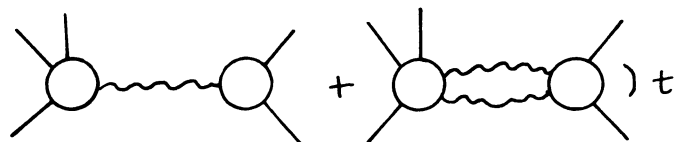
(b)

Fig. 5.7

Fig.5.8

Fig. 5.9

Fig. 5.10